

AD-A267 692



12

NSWCDD/TR-92/206

**INVESTIGATION OF THE ORIGIN OF HOT SPOTS IN
DEFORMED CRYSTALS: FINAL REPORT ON
AMMONIUM PERCHLORATE STUDIES**

BY W. L. ELBAN (LOYOLA COLLEGE)
H. W. SANDUSKY B. C. BEARD B. C. GLANCY (NSWCDD)

RESEARCH AND TECHNOLOGY DEPARTMENT

19 JULY 1993

Approved for public release; distribution is unlimited.

DTIC
ELECTE
AUG 04 1993
S A D



NAVAL SURFACE WARFARE CENTER
DAHLGREN DIVISION • WHITE OAK DETACHMENT

Silver Spring, Maryland 20903-5640

424 565
93-17473



4036

93 8 3 183

INVESTIGATION OF THE ORIGIN OF HOT SPOTS IN DEFORMED CRYSTALS: FINAL REPORT ON AMMONIUM PERCHLORATE STUDIES

BY W. L. ELBAN (LOYOLA COLLEGE)
H. W. SANDUSKY B. C. BEARD B. C. GLANCY (NSWCDD)
RESEARCH AND TECHNOLOGY DEPARTMENT

19 JULY 1993

Accession For	
NTIS CRA&I	<input checked="checked" type="checkbox"/>
DTIC TAB	<input type="checkbox"/>
Unannounced	<input type="checkbox"/>
Justification	
By	
Distribution /	
Availability Codes	
Dist	Avail and/or Special
A-1	

Approved for public release; distribution is unlimited.

DTIC QUALITY INSPECTED 3

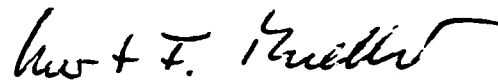
NAVAL SURFACE WARFARE CENTER
DAHLGREN DIVISION • WHITE OAK DETACHMENT
Silver Spring, Maryland 20903-5640

FOREWORD

This work was performed to determine the role that material microstructure has on the shock reactivity of ammonium perchlorate (AP) single crystals. Diamond pyramid (Vickers) indentation hardness testing revealed that AP plastically deforms readily with a significant release of strain energy. Slip and cracking systems extend well beyond the size of the hardness impressions. It was shown that decomposition is enhanced in preexisting regions of increased dislocation density when shocked near the reaction threshold. These zones of enhanced decomposition preferentially extend along a slip or cracking system, depending on crystal orientation when shocked. Furthermore, the threshold of reaction and the material response of the shocked crystals were a function of orientation. The results are significant for understanding how defects in AP crystals can enhance the reactivity of a composite energetic material, containing AP, when subjected to shock or impact.

The work was supported by the Office of Naval Research under work request numbers N00014-87-K-0175 and N00014-85-WR-24103 as a cooperative effort between Loyola College, Baltimore, and the Naval Surface Warfare Center, White Oak Detachment (NSWCWODET). Support was also provided by the Independent Research Program at NSWCWODET. Drs. Richard R. Bernecker (NSWCWODET) and Sigmund J. Jacobs (Advanced Technology and Research, Inc., Laurel, Maryland) provided many helpful comments and guidance concerning the early direction of the work. Dr. Bernecker also provided an extensive review of the current report. Numerous helpful discussions were held with Prof. Ronald W. Armstrong (Department of Mechanical Engineering, University of Maryland, College Park (UMCP)). Large (> 1 cm), optical quality, pure single crystals of AP were provided by T. L. Boggs (Naval Air Warfare Center, China Lake, California). Dorn W. Carlson and Sybil S. Turner (NSWCWODET) performed the liquid ion chromatography (LIC) analysis on recovered crystals. Dr. Marriner K. Norr (NSWCWODET) obtained the low magnification scanning electron microscope (SEM) photographs in Figure 9. Prof. Donald A. Keefer (Department of Biology, Loyola College) helped with the transmission light microscopy used to obtain Figure 3(A). Dr. Xian Jie Zhang (UMCP) printed the photograph appearing in Figure 3(A). Dr. James P. Ritchie (Los Alamos National Laboratory, Los Alamos, New Mexico) provided the calculations of the changes in chlorine energy levels in response to geometric and bond length variations in the perchlorate anion.

Approved by



KURT F. MUELLER, Head
Explosives and Warhead Division

ABSTRACT

A number of single crystals of ammonium perchlorate (AP) were shock loaded near the reaction threshold to investigate the effects of concentrated lattice defects (dislocations) and differing crystal orientations on chemical reactivity. Large, optical quality crystals of pure AP were immersed in mineral oil and shocked through either the (001) or $\{2\bar{1}0\}$ surfaces by a detonator. Prior to shock loading, some crystals had localized regions of increased lattice defects and strain created by placing diamond pyramid (Vickers) hardness impressions into their exterior cleavage surfaces. High-speed photographs showed preferential cracking and luminosity near some of the hardness impressions. The photographs also revealed the occurrence of the same slip deformation identified previously from hardness testing. The shocked crystals were recovered, sometimes intact, for microstructural characterization and chemical analyses. Crystal orientation relative to the shock propagation direction changed the dynamic response and threshold for decomposition of the crystal, indicating the influence of material microstructure. Similarly, placing the hardness indenter in various surfaces of unshocked crystals activated different slip and cracking systems. One recovered crystal was cleaved twice through hardness impressions on the (001) and shock-entry ($2\bar{1}0$) surfaces, allowing spatial analysis of the interior regions of the crystal using x-ray photoelectron spectroscopy (XPS). Along these freshly cleaved surfaces, the XPS results showed enhanced lattice disruption and perchlorate decomposition as a result of the hardness impressions. The greatest decomposition was not immediately adjacent to the impressions, but near the tips of cracks and along slip planes emanating from the impressions several millimeters, or more, into the crystal.

CONTENTS

	<u>Page</u>
INTRODUCTION	1
EXPERIMENTAL APPROACH AND TECHNIQUES	2
CRYSTAL DEFORMATION AND MICROSTRUCTURAL CHARACTERIZATION ...	4
SHOCK LOADING	5
CHEMICAL ANALYSIS	5
EXPERIMENTAL RESULTS	8
VICKERS HARDNESS STUDIES	8
SHOCK LOADING STUDIES	9
MICROSTRUCTURAL CHARACTERIZATION OF RECOVERED CRYSTAL	
FROM SHOT ONR-35	17
XPS ANALYSIS OF RECOVERED CRYSTAL FROM SHOT ONR-35	17
ADDITIONAL XPS RESULTS	21
DISCUSSION	22
SUMMARY AND CONCLUSIONS	25
REFERENCES	27
DISTRIBUTION	(1)

ILLUSTRATIONS

<u>Figure</u>		<u>Page</u>
1	SCALE DRAWING OF AP CRYSTAL USED IN SHOT ONR-35	3
2	ARRANGEMENT FOR SHOCK LOADING AP CRYSTAL IMMERSED IN MINERAL OIL SHOWING FIELD OF VIEW FOR FRAMING CAMERA, SHOT ONR-35	7
3	DIAMOND PYRAMID (VICKERS) HARDNESS IMPRESSIONS IN {210} SURFACES OF AP CRYSTALS	10
4	FORCE VERSUS DIAGONAL AND CRACK LENGTHS FOR DIAMOND PYRAMID (VICKERS) IMPRESSIONS IN (210) OR (210) SURFACES OF AP CRYSTALS	11
5	PHOTOMACROGRAPHS OF EXTERIOR (001) SURFACE OF AP CRYSTAL BEFORE AND AFTER SHOCK ENTRY INTO (210) SURFACE, SHOT ONR-35	13
6	PHOTOMACROGRAPHS AND SCHEMATIC OF (001) SURFACE OF AP CRYSTALS AFTER SHOCK ENTRY INTO THAT SURFACE	14
7	BACKLIT FRAMING CAMERA PHOTOGRAPHS OF (001) SURFACE OF AP CRYSTAL SHOCKED TO 24.4 KBAR, SHOT ONR-35	15
8	REFLECTED LIGHT PHOTOMICROGRAPH OF SLIP TRACES AND CRACKING NEAR CENTER OF EXTERIOR (001) SURFACE OF RECOVERED AP CRYSTAL, SHOT ONR-35	18
9	LOW MAGNIFICATION SEM PHOTOGRAPHS OF CRACKING IN VICINITY OF (210) VICKERS HARDNESS IMPRESSION IN RECOVERED AP CRYSTAL, SHOT ONR-35	19
10	XPS ANALYSIS RESULTS FROM INTERIOR OF AP CRYSTAL SHOCKED TO 24.4 KBAR, SHOT ONR-35	20
11	SCHEMATIC OF VARIOUS FEATURES VIEWED ON OR THROUGH (001) SURFACE OF RECOVERED AP CRYSTAL, SHOT ONR-35	23

TABLES

<u>Table</u>		<u>Page</u>
1	SELECTED SHOCK LOADING EXPERIMENTS	6

INTRODUCTION

Deformation, fracture, and material microstructure are important aspects of the shock reactivity of ammonium perchlorate (AP) single crystals. In previous work,¹ large (> 10 mm on an edge), optically transparent crystals were cleaved into samples with edge dimensions varying from 3 to 10 mm. The orientations of the resultant cleavage surfaces were verified using the Laue back-reflection x-ray diffraction technique. Preparatory to the shock-loading experiments, diamond pyramid (Vickers) microindentation hardness testing (loads ranged from 0.0981 to 0.981 N) was performed on the (001) surface of an unshocked AP crystal.¹ Surface traces of slip planes and cracks associated with the hardness impressions were crystallographically identified. This allowed determination of the indentation-forming (primary deformation) and volume-accommodating (secondary deformation) slip systems. The easiest operative system was (100)[001]. Particularly noteworthy was the observation that cracking occurred in the region of greatest plastic deformation. When indenter force was correlated with indentation diagonal and resultant crack lengths, the hardness was observed to decrease with increasing force, which was attributed to the occurrence of cracking.

In a series of shock-loading experiments, the crystals were oriented such that the shock from a small explosive donor entered the {210} surface, allowing the orthogonal (001) surface to be photographed by a high-speed framing camera.¹ The crystals were immersed in a mineral oil bath, and shock loaded at peak pressures ranging from 1 to 38.5 kbar. Prior to shock loading, two crystals each had a large surface defect created by putting a Vickers hardness indenter into the (001) surface with a load of 9.81 N. The crystals were recovered, sometimes intact, for quantitative analysis of chemical decomposition using liquid ion chromatography (LIC). One recovered crystal was also characterized for microstructural changes using light microscopy and Vickers microindentation hardness testing.

A reaction threshold of ~ 25 kbar was established by performing analysis of decomposition products in recovered pieces of shocked AP crystals using LIC.¹ Although successful in measuring bulk chemical reaction, this technique did not provide spatially specific information. Reactivity results of this type would have been particularly desirable because high-speed photographs taken during one of the shock experiments showed luminosity, presumably associated with chemical reaction, in the vicinity of a large (001) surface impression. The high-speed photographs also revealed, although not in each experiment, a luminous shock front, distinct diagonal lines immediately behind the front that were attributed to the (010)[001] secondary slip system, and a moving luminous band that appeared to be a propagating crack. Near the threshold, it appears that reaction in even relatively defect-free AP crystals is inhomogeneous, being directly related to the material microstructure.

Vickers microindentation hardness testing was performed to probe the strength of one of the shocked AP crystals that was recovered intact.¹ This crystal was cloudy in appearance, and microscopic examination of the external (001) surface revealed that extensive ($\bar{1}00$) and (010) slip trace formation had occurred. Slip on these planes corresponds to the primary and secondary deformation, respectively, in forming Vickers hardness impressions in the (001) surface of an unshocked crystal. The hardness and cracking properties of the shocked crystal varied depending on the location of the probing hardness impressions. The greatest increase in hardness was measured in the region of the crystal that initially experienced shock wave passage. A smaller hardness increase was measured at the intersection of ($\bar{1}00$) and (010) slip traces. Radial crack extension at the fresh hardness impressions was generally reduced. The combined results indicated that shock loading did work harden AP and that the shock-induced microstructure made crack propagation more difficult.

The purpose of the current work is two-fold. First, a set of experiments, complementing the initial set of experiments, was performed to investigate the effect of crystal orientation on the shock reactivity of AP. Crystals were now oriented so that the shock entered the (001) surface, which is orthogonal to the shock propagation direction in the previous experiments. High-speed framing camera photographs were taken of the ($\bar{2}10$) surface, which normally contained at least one Vickers hardness impression, and chemical analysis was performed on the recovered crystals using LIC. Second, a small number of additional experiments was conducted on crystals shocked in the original propagation direction, perpendicular to the ($\bar{2}10$) surface, while the indented (001) surface was viewed with the framing camera. These experiments were performed to obtain spatially specific chemical analysis results using x-ray photoelectron spectroscopy (XPS) to elucidate whether decomposition is dependent on material microstructure.

EXPERIMENTAL APPROACH AND TECHNIQUES

The effect of material microstructure on the shock reactivity of AP single crystals was investigated by two approaches. One approach was to determine the effect of crystal orientation relative to shock propagation direction on reaction threshold. This was of interest because previous low strain-rate Vickers indentation hardness testing revealed^{2,3} that different slip and cracking systems were involved in accommodating the indenter on the two surfaces. The other approach involved frequently putting relatively large strain centers into the surfaces by Vickers testing prior to shock loading. Hardness impressions provided localized concentrations of crystal lattice defects (dislocations) in a controlled manner. The cumulative dislocation strain fields of the hardness impressions should exhibit enhanced chemical reaction.^{4,5} The impressions would also serve as sites to concentrate additional plastic deformation and cracking during shock loading, hence increasing the possibility of a further contribution to chemical decomposition.

The current shock experiments were performed on cleaved sections of optical quality, single crystals of AP that came from the same lot of crystals studied previously.^{1,2} Figure 1 is a three-dimensional scale drawing of the crystal section used in an experiment, designated as Shot ONR-35, and is representative of the other crystals that were shocked. ONR-35 was a continuation of the previous experiments in which the (001) surface was viewed following shock entry into the orthogonal ($\bar{2}10$)

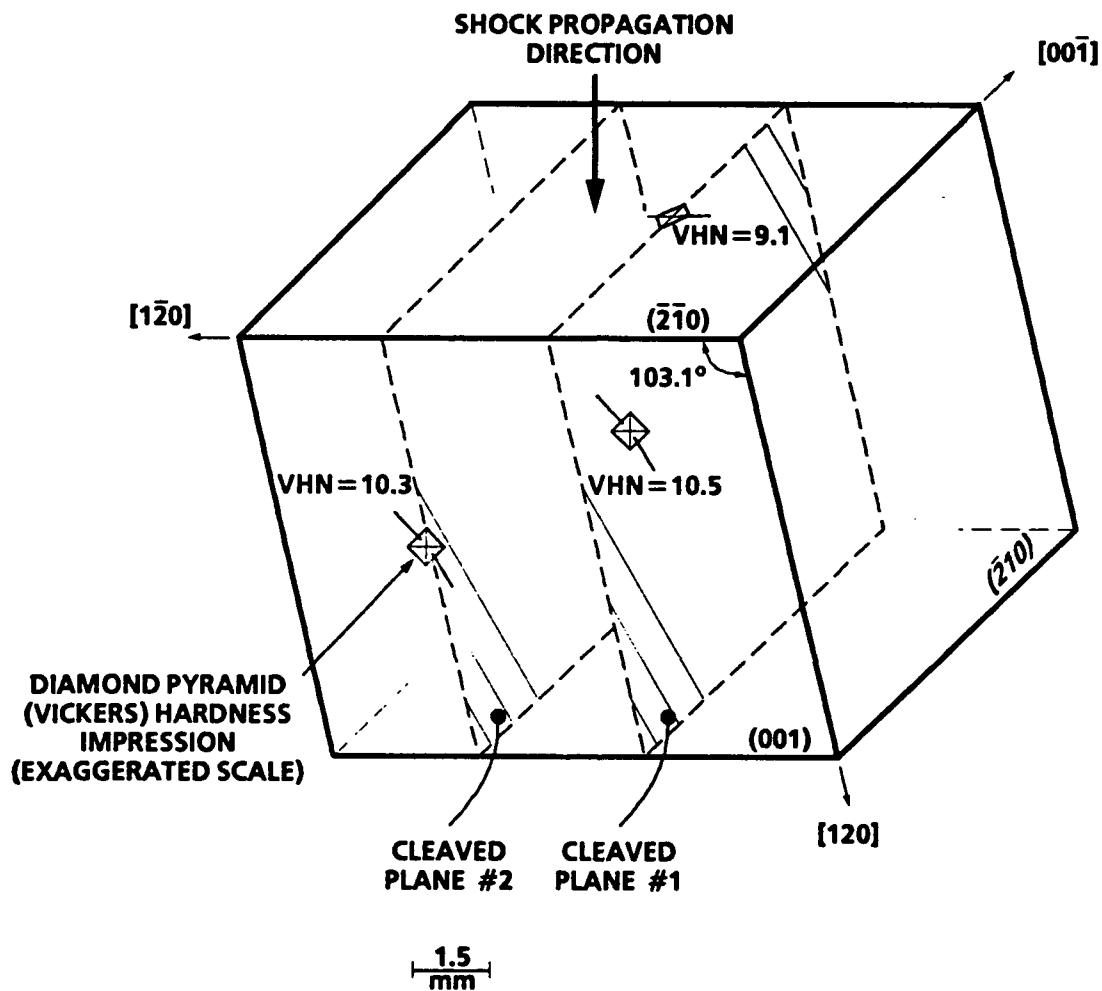


FIGURE 1. SCALE DRAWING OF AP CRYSTAL USED IN SHOT ONR-35

surface. The crystals in most of the other experiments were oriented for shock entry into the (001) surface while viewing the orthogonal ($\bar{2}10$) surface. Figure 1 shows crystallographic information and the positions of Vickers impressions. The locations are also given for two freshly cleaved planes in the shocked crystal that was recovered intact. These planes were chosen to pass through the hardness impressions in order to perform chemical analysis and microstructural characterization of the crystal interior within the strain fields underneath these impressions.

CRYSTAL DEFORMATION AND MICROSTRUCTURAL CHARACTERIZATION

Prior to the shock-loading experiments, Vickers microindentation hardness testing was performed at low strain rate on the ($\bar{2}10$) surface.^{2,3} This was accomplished using a LECO model M-400 microhardness tester with loads ranging from 0.0981 to 0.981 N for a dwell time of 20 s. The residual impressions were examined primarily in transmitted light and polarized transmitted light with a Zeiss Photomicroscope. The impressions were analyzed to obtain information about slip and cracking systems as well as the size and character of the strain fields surrounding the impressions. Also, the effect of cracking on hardness with increasing applied load was determined to assess the case of strain energy dissipation. Microstructural characterization of the impressions was necessary to understand the effect of the resultant strain fields on shock reactivity. Further, the expectation was that many of the same deformation systems involved at low strain rate would be active at the high rates experienced during shocking. The spherically diverging wave front in the shock experiments is conceptually similar to performing a conventional indentation hardness test with a large ball, except that the strain rate for shocking is orders of magnitude greater. A diverging shock, in contrast to a planar shock, permitted the desired activation of slip and cracking systems.

In the current work, Vickers hardness testing at loads >0.981 N was performed on the ($\bar{2}10$) surface of other AP crystals using a Tukon model FB tester with a dwell time ≥ 17 s. One or more exterior surfaces of the majority of the shock-loaded crystals had at least one impression (9.81 N load, typically). The impressions resulting at this load are considered to be of sufficient scale for observing their effect in the shock-loading experiments. The size of the plastic impressions with accompanying cracks was sufficiently large to be studied and photographed more appropriately using a Zeiss Tessovar photomacrographic zoom system (41X maximum magnification). Measurement of the impression diagonal and crack lengths were obtained using the microscope capability (i.e., Filar micrometer eyepiece attachment) of the Tukon tester and from photomacrographs.

The microstructural state of crystals recovered from the shock experiments was also assessed. The crystals were washed in heptane to remove residual mineral oil, and optical microscopy was performed on the crystal exterior and several freshly cleaved surfaces. In addition to using the Zeiss Tessovar system, a Zeiss model ICM 405 bench metallograph was employed, allowing surfaces to be viewed at magnifications up to 1000X with reflected light brightfield illumination and using Nomarski differential interference contrast. Freshly cleaved surfaces were also examined at low magnification ($<50X$) with an Advanced Metals Research Corporation (AMR) model 1000A scanning electron microscope (SEM).

SHOCK LOADING

Conditions for selected shock-loading experiments are given in Table 1. The experiments used a closed chamber filled with mineral oil and having ports for backlighting and photographic viewing. This arrangement and the calibration of the shock pulse in the mineral oil have been discussed previously.^{1,2} Figure 2 shows the most significant aspects of the setup within the closed chamber for Shot ONR-35, including the field of view of the high-speed camera. This setup was used throughout, except for changes in crystal orientation and separation distance from the detonator. The shock was generated by a Reynolds RP-80 detonator containing an explosive pellet in a Delrin (polyoxymethylene polymer) sleeve with no bottom covering. The exposed bottom (output end) of the explosive pellet was sealed by grease. The detonator was positioned directly above the crystal, which was supported on clear tape above a block of oil-soaked polyurethane foam. Immersing the crystal in oil and capturing it in the foam permitted "soft" recovery of most of each crystal for subsequent chemical analysis and microstructural characterization.

The optical quality of the as-cleaved surfaces and bulk transparency of the crystal (discussed later) permitted in-depth viewing as well as transmission of the backlighting. The view of the crystal was relatively undisturbed by shock passage before being obscured by gaseous detonator products $\sim 5 \mu\text{s}$ later. As shown in Figure 2, the crystal occupied most of the backlit field of view of the Imacon Model 790 image converter camera. The high-speed photographs shown in Reference 1 were recorded at rates of 2 or 5 million frames per second (fps) on Polaroid instant print film with a speed of ISO 3000. In Shot ONR-35, the framing rate was reduced to 1 million fps in order to observe events several microseconds after shock passage. Also in Shot ONR-35, Kodak TMAX 400 negative film was used to improve resolution, which enabled detection of some previously unseen details.

CHEMICAL ANALYSIS

Crystals shocked perpendicular to the (001) surface were analyzed for bulk chemical decomposition by LIC, as in the previous study.^{1,2} This was done to determine the onset and extent of reaction as a function of shock pressure for this second propagation direction. In addition, two crystals shocked perpendicular to the $\{210\}$ surface were analyzed to augment earlier LIC results.

XPS, with an approximate sampling area of 1 mm x 1 mm, was used as a second analysis technique. Considerable effort was devoted to studying the crystal from Shot ONR-35. The crystal was recovered intact and subsequently cleaved through the impressions in both surfaces (Figure 1), providing two fresh $\{210\}$ surfaces for analysis. This approach provided a means to analyze the crystal interior with the necessary spatial resolution to determine quantitatively whether significant chemical decomposition occurred preferentially in the vicinity of the hardness impressions as a result of shock loading. Cleaving the recovered crystal just prior to XPS analysis further avoided the complicating effect of exterior surface contamination.

A series of XPS spectra of the two freshly cleaved surfaces taken from the Shot ONR-35 crystal were collected using a Physical Electronics 5400 photoelectron spectrometer. The characterization was performed with a monochromatized Al x-ray source, operated at 600 W (15 KV, 40 ma). A monochromatized source was used

TABLE 1. SELECTED SHOCK LOADING EXPERIMENTS

Shot Surfaces ONR- with VHIs ¹	Gap (mm)	Shock Pressure in Oil/AP (kbar)	AP Post-Shock Condition	Post-Shock Chemical Analysis LIC Measurements (ppm)			
				Cl ⁻	NO ₂ ⁻	NO ₃ ⁻	ClO ₃ ⁻
UNSHOCKED CONTROL WITH VHI				420	8	46	4
SHOCK ENTRY INTO {210} SURFACE, VIEWING (001) SURFACE							
19 [*] (001)	7.0	10.5/16.7	Intact but cloudy (Photographs and results of hardness tests in Ref. 1)	-	-	-	-
17	-	6.0	15.5/24.4	Broke into two pieces	One piece: 1,400	6	60
					Other piece: 900	18	20
18 ⁺⁺ (001)	6.0	15.5/24.4	61 wt% recovered	Large piece divided into sections	1,100	33	83
					1,700	30	136
28 (001)	6.0	15.5/24.4	75 wt% recovered		-	-	-
35 (001) & {210}	6.0	15.5/24.4	Intact (Figure 5)		XPS analysis (Figure 10)		
16 [*] -	5.0	24.8/38.5	88 wt% recovered		11,000	8	46
24 -	5.0	24.8/38.5	Intact with large plastic deformation		XPS analysis		
27 -	4.0	40.6/62.5	58 wt% recovered in five pieces	Large piece divided into sections	1,700	52	260
				Another piece:	3,300	36	81
					1,300	15	140
SHOCK ENTRY INTO (001) SURFACE, VIEWING {210} SURFACE							
30 {210}	7.0	10.5/16.7	83 wt% recovered in four pieces		735	35	103
29 {210}	6.0	15.5/24.4	91 wt% recovered in four pieces		625	78	106
31 -	5.0	24.8/38.5	Fully recovered in two pieces		-	-	-

* High-speed photographs shown in Reference 1

[#] VHI = Vickers hardness impression⁺ Detonator positioned over viewed surface instead of centered over crystal

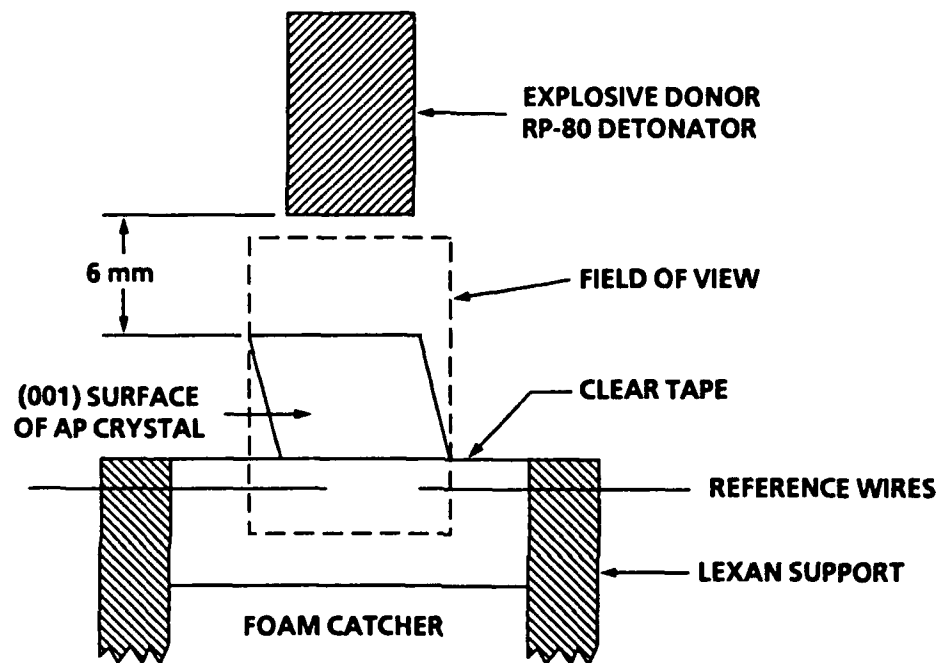


FIGURE 2. ARRANGEMENT FOR SHOCK LOADING AP CRYSTAL IMMERSSED IN MINERAL OIL SHOWING FIELD OF VIEW FOR FRAMING CAMERA, SHOT ONR-35

because it offered the following advantages. First, the highly refined energy distribution produces narrower photoelectron peaks, thereby improving the spectral resolution. Next, radiation damage is greatly reduced as all of the extraneous Brehmstrahlung x-ray radiation and high electron background are eliminated. Finally, satellite photoelectron peaks excited by the $K\alpha_{3,4}$ x-ray lines do not appear. This simplifies the identification of new chemical states at binding energies 8-12 eV below the major component in the spectrum, such as in the chlorine spectra from AP.

Radiation damage of the AP crystal was avoided by trading off spectral quality against extended analysis times. Investigation of the sensitivity of AP to the monochromatic x-ray source showed that an exposure time greater than 15 minutes is required before any noticeable changes in Cl(2p) line shapes are observed. Analysis time at each spot was never more than 5 minutes and typically was about 3 minutes. Although the instrument has the capability of analyzing a spot size of 200 μm , the 1 mm spot size used in this work was chosen to minimize the analysis time and thereby the possibility of radiation damage.

Binding energy values were referenced to 285.0 eV for the carbon (1s) peak from hydrocarbon contamination inevitably present on the surface of a sample prepared outside the vacuum chamber. Charge accumulation on the surface of the insulating samples was compensated for by a low energy electron flood source. Spectra were collected under conditions that produce a full width of peak at half maximum height (FWHM) of 1.03 eV for the 3d 5/2 line from pure sputtered silver. Chlorine (2p), nitrogen (1s), and carbon (1s) XPS spectra were collected at each analysis spot on the cleaved surfaces. Curve fitting of these spectra was performed using a Gaussian/Lorentzian line shape superimposed on an integrated background.

Prior to the detailed study of the crystal from Shot ONR-35, some XPS measurements were obtained on the intact, but highly deformed, crystal recovered from Shot ONR-24. This crystal was without hardness impressions, in contrast to Shot ONR-35, but was shocked to a higher pressure of 38.5 kbar. Spectra were obtained on two freshly cleaved surfaces: (1) the mid-plane parallel to the {210} shock-entry surface and (2) a {210} surface that formed in the top half of the crystal during the cleaving operation to create the first surface.

An additional benefit from the use of XPS was the discovery of the relationship between spectral line widths and the degree of microstructural perfection. Variations in the observed line widths were correlated^{6,7} with changes in visible damage (i.e., degree of cloudiness) and increased dislocation densities throughout the shocked crystal. The line broadening results will be discussed briefly and related to decomposition.

EXPERIMENTAL RESULTS

VICKERS HARDNESS STUDIES

Crystallographic information on slip and cracking systems obtained from Vickers microindentation hardness testing (loads ≤ 0.981 N) of the (001) and (210) surfaces of AP single crystals has been previously described in detail.¹⁻³ A transmitted light photomicrograph^{2,3} of an impression put into the (210) surface at

0.981 N load appears in Figure 3(A). Particularly noteworthy is the $(00\bar{1})$ crack that extends from the top corner of the impression. In addition, slip traces, such as the identified $(\bar{1}1\bar{1})$, are clearly seen intersecting the $(\bar{2}10)$ surface beyond the asymmetric four facets of the impression.

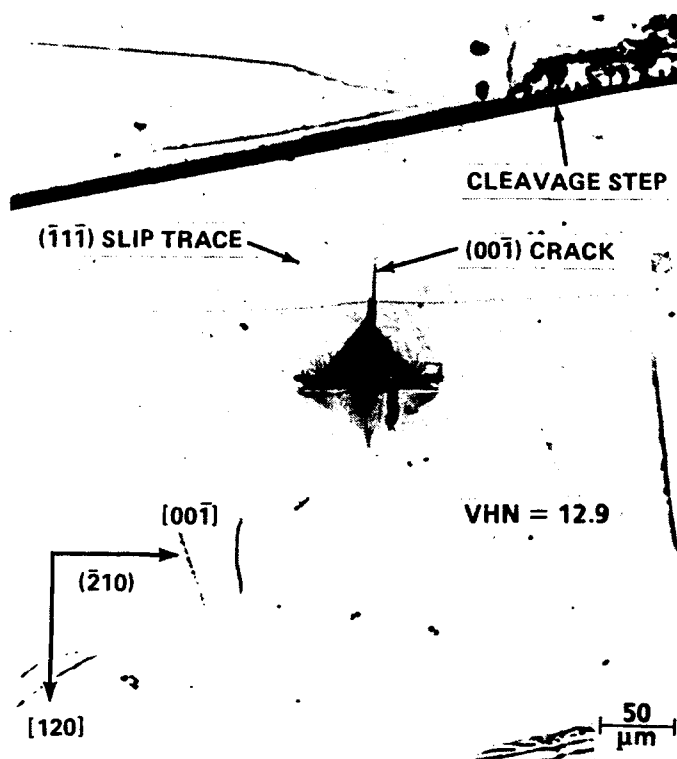
A reflected light photomicrograph of a Vickers impression (9.81 N) that was put into the $(\bar{2}10)$ surface of the crystal used in Shot ONR-35 appears in Figure 3(B). This photomicrograph has been rotated 90° , relative to Figure 3(A), to connect directly with the crystal orientation in Figure 1. The expectation is that the deformation should be the same for indentations put into either the $(\bar{2}10)$ or $(\bar{2}\bar{1}0)$ surface. However, other deformation systems could be activated at higher loads. This is observed when comparing the indentations from 0.981 and 9.81 N loads in Figures 3(A) and 3(B), respectively. For the impression in Figure 3(B), a second branch of the $(00\bar{1})$ crack is also present, along with prominent cracking that is inclined to the $(\bar{2}10)$ surface. The second $(00\bar{1})$ crack branch is obscured in Figure 3(B) by scattered light from the inclined crack planes.

A comparison of Vickers hardness numbers (VHNs), expressed in standard units of kgf/mm^2 , for the impressions in Figures 3(A) and 3(B) reveals that a 29.5 percent decrease in hardness occurred as the load was increased from 0.981 to 9.81 N. This trend is consistently maintained for all of the hardness data obtained for Vickers impressions primarily put in the $(\bar{2}10)$ surface but including one in the $(\bar{2}\bar{1}0)$ shock-entry surface of Shot ONR-35. The combined results for all of the crystals tested are given in Figure 4 as a logarithmic plot of force on the indenter versus indentation diagonal and $(00\bar{1})$ crack lengths for forces ranging from 0.0981 to 9.81 N. Two distinct regimes in the data can be seen, resulting from the appearance of the second branch of the $(00\bar{1})$ crack at 0.981 N. Below 0.981 N, a slope of 1.91 for the indentation diagonal length data was obtained compared to a value of 2.0 for constant hardness behavior. The emergence of the second $(00\bar{1})$ crack branch above 0.981 N causes a much greater difference, 1.60 versus 2.0. By comparison, the diagonal length data reported¹ for Vickers impressions put into the (001) surface yielded a single straight line with a slope of 1.87. The decrease in hardness for both surfaces, as indicated by slopes of <2.0 , is attributed to cracking which causes a sizeable strain energy release.

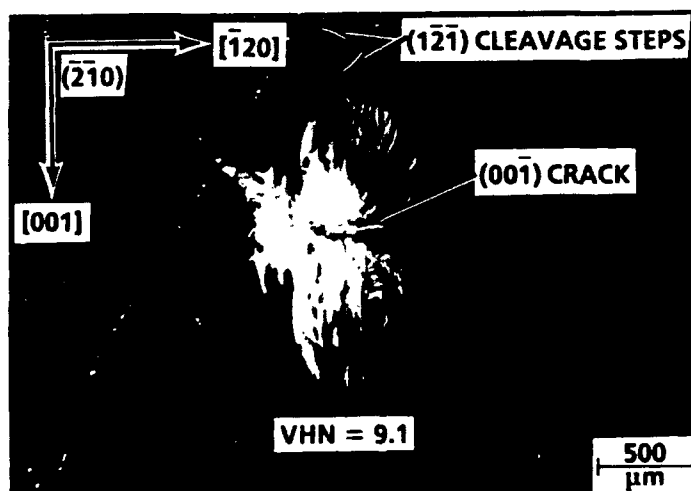
Although somewhat scattered, the $(00\bar{1})$ crack length data were fit to two displaced, straight line segments each having a slope of 1.5. A force-crack length dependency having this slope is obtained from indentation fracture mechanics analyses.^{8,9} The horizontal displacement in the crack length data is also associated with the appearance of the second branch of the $(00\bar{1})$ crack. Such a shift indicates that the coefficient in the fracture mechanics power law dependency (i.e., the indentation fracture mechanics stress intensity¹⁰) has been diminished by the appearance of the second crack branch. The stress intensity is proportional to $(E\gamma)^{1/2}$, where E is Young's modulus and γ is the fracture surface energy.¹⁰ A dislocation reaction mechanism has been proposed to explain $(00\bar{1})$ crack formation as slip-induced cleavage.^{2,3} As such, it appears that the increased deformation that occurs at higher loads assists the $(00\bar{1})$ cracking.

SHOCK LOADING STUDIES

The results of selected experiments for shock entry into either the $\{\bar{2}10\}$ or (001) surfaces are summarized in Table 1. The reaction threshold for shock entry into the $\{\bar{2}10\}$ surface was established¹ to be ~ 25 kbar (shock pressure in the crystal, P_{Ap}) using



(A) 0.981 N LOAD ON $\{210\}$ SURFACE



(B) 9.81 N LOAD ON $\{210\}$ SURFACE BEFORE SHOCK LOADING, SHOT ONR-35

FIGURE 3. DIAMOND PYRAMID (VICKERS) HARDNESS IMPRESSIONS IN $\{210\}$ SURFACES OF AP CRYSTALS

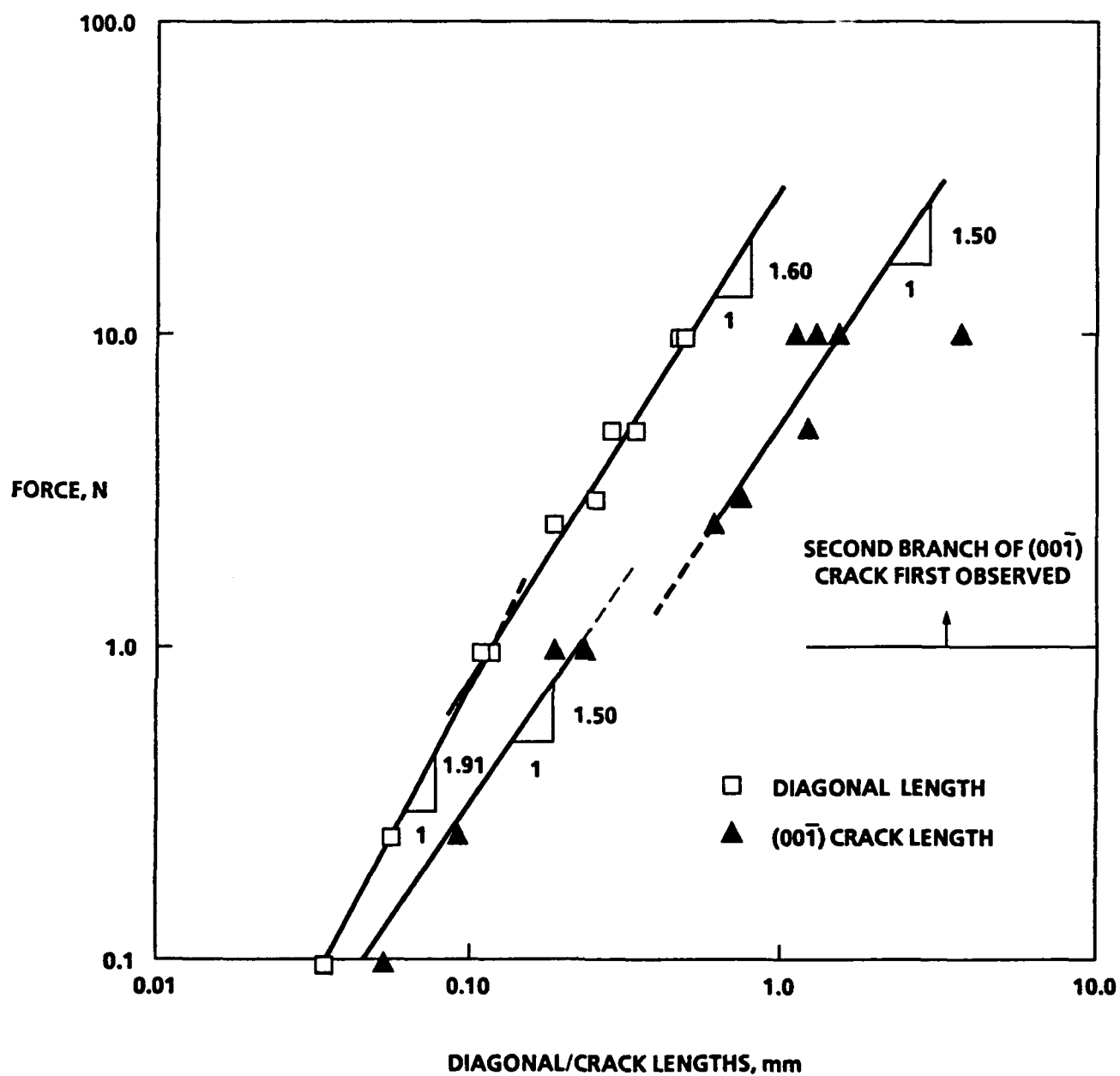


FIGURE 4. FORCE VERSUS DIAGONAL AND CRACK LENGTHS FOR DIAMOND PYRAMID (VICKERS) IMPRESSIONS IN $(\bar{2}10)$ OR $(\bar{2}\bar{1}0)$ SURFACES OF AP CRYSTALS ($[00\bar{1}]$ DIAGONAL)

LIC analysis results. Only the Cl^- concentration showed a significant change relative to an unshocked crystal. There was little consistent change in measurements for NO_2^- , NO_3^- , and ClO_3^- up to $P_{\text{AP}} = 38.5$ kbar.¹ A second attempt at obtaining LIC results for the crystal recovered from Shot ONR-18 was successful and yielded consistent values with those reported previously¹ for the Shot ONR-17 crystal. In a recent experiment with $P_{\text{AP}} = 62.5$ kbar (Shot ONR-27), there was a large decrease in Cl^- relative to that obtained for $P_{\text{AP}} = 38.5$ kbar, but significant increases in NO_2^- and NO_3^- . (No measurements for ClO_3^- were made on recovered crystals from the recent experiments.) Crystals from recent experiments with shock entry into the (001) surface also had significantly increased NO_2^- and NO_3^- , in addition to Cl^- , for $P_{\text{AP}} = 16.7$ and 24.4 kbar (Shots ONR-30,29). There were insufficient experiments to establish precisely the reaction threshold for shock entry into the (001) surface. The threshold appears to be less than or equal to 16.7 kbar, which is below that for shock entry into the $\{210\}$ surface.

The damage resulting from shock loading the AP crystal in Shot ONR-35 to 24.4 kbar can be seen relative to the unshocked crystal in the photomicrographs in Figure 5. The shocked crystal (Figure 5(B)) has nonuniform cloudiness which is most intense at the $(\bar{2}10)$ shock-entry surface. The degree of cloudiness lessened with distance from the entry surface, correlating roughly with the attenuation of shock pressure. However, the boundary between the cloudy and clear regions is not spherical (or circular as viewed through the (001) surface), as might be expected from a spherically diverging shock front. The bottom region of the crystal is still transparent, having the appearance of the unshocked crystal in Figure 5(A). Although insufficient to cause cloudiness, some microscopic damage did occur in the bottom region. A chemical etch pitting study yielded a dislocation density of $3.0 \times 10^5 \text{ cm}^{-2}$ for the bottom region versus $0.82 - 1.4 \times 10^5 \text{ cm}^{-2}$ for an unshocked crystal (control).⁷ The dislocation density increased to $1.2 \times 10^6 \text{ cm}^{-2}$ in the center region of the recovered crystal where significant cloudiness was present. It was not possible to measure dislocation densities in the top half of the crystal because of the severe surface roughness resulting from cleaving.

Less cloudiness was observed in the recovered AP crystals shocked through the (001) surface (Figure 6). None of the crystals from this abbreviated test sequence listed in Table 1 remained intact. Two of the crystals (Shots ONR-29,30) were recovered in four, roughly equal-sized pieces. The crystals exhibited $(\bar{2}10)$ cleavage cracking and cracking on (110). Shot ONR-31 was recovered initially intact but readily broke into two pieces on handling. The fracture was more complex in appearance, being predominantly (230). In another experiment (Shot ONR-34), which is not listed in Table 1, the crystal was subjected to the same shock pressure ($P_{\text{AP}} = 24.4$ kbar) as in Shot ONR-29 but remained intact. The crystals in Shots ONR-31,34 were slightly larger than the crystals which fractured into four pieces in Shots ONR-29,30. Thus, it appears that the extent of fracturing is reduced for a larger crystal in which rarefactions overtake the attenuated shock at a point farther from entry.

High-speed framing photographs from Shot ONR-35 are shown in Figure 7 for the field of view outlined in Figure 2. The times associated with each frame are relative to the first frame, which was taken after the shock from the detonator had crossed the mineral oil gap and just entered the crystal at 24.4 kbar. In the first frame (0.0 μs), the shock in the crystal is noticeably curved and has a higher velocity than in the oil. The backlighting continues to be transmitted through the crystal behind the shock, whereas the 15.5 kbar shock in the oil deflects the backlighting. Thus, there is a narrow zone between the two fronts which permits viewing the

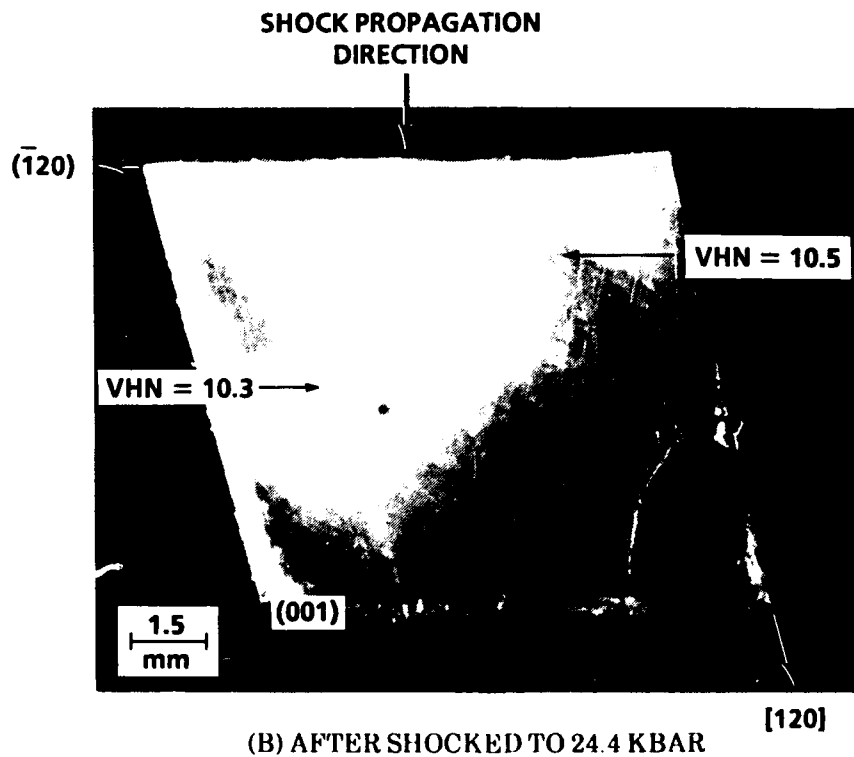
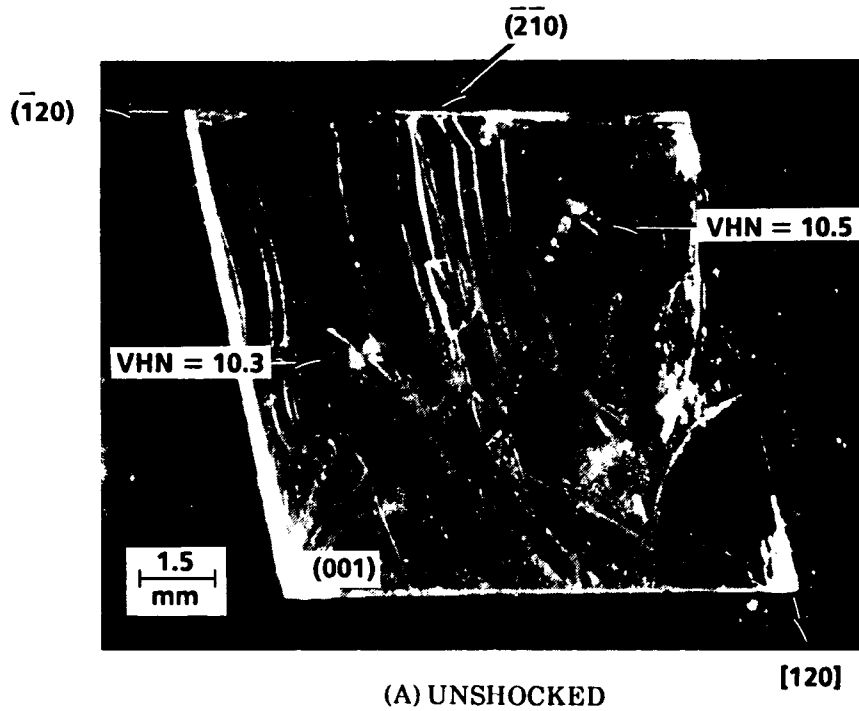
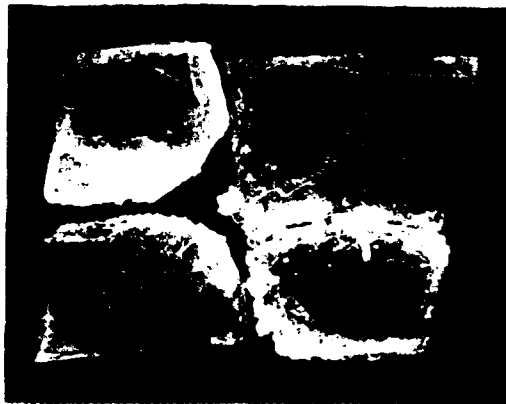
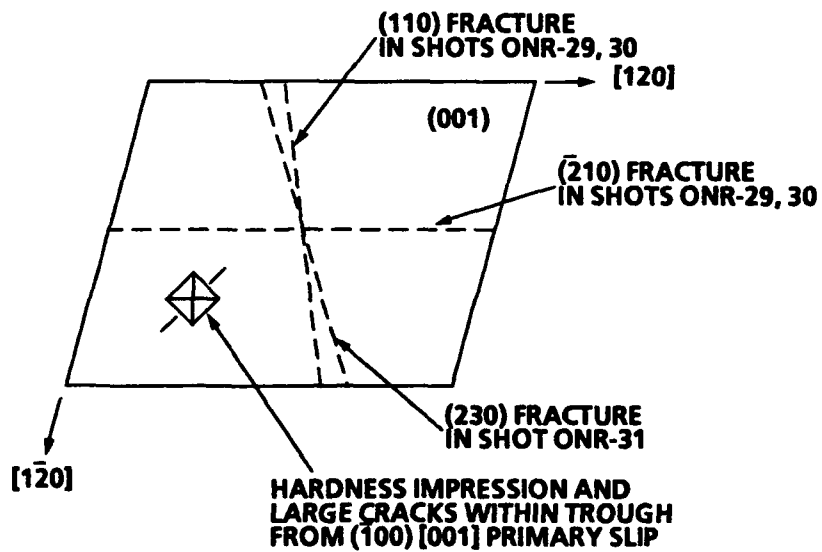


FIGURE 5. PHOTOMACROGRAPHS OF EXTERIOR (001) SURFACE OF AP CRYSTAL BEFORE AND AFTER SHOCK ENTRY INTO $(\bar{2}10)$ SURFACE, SHOT ONR-35



(A) AFTER SHOCKED TO 24.4 KBAR, SHOT ONR-29

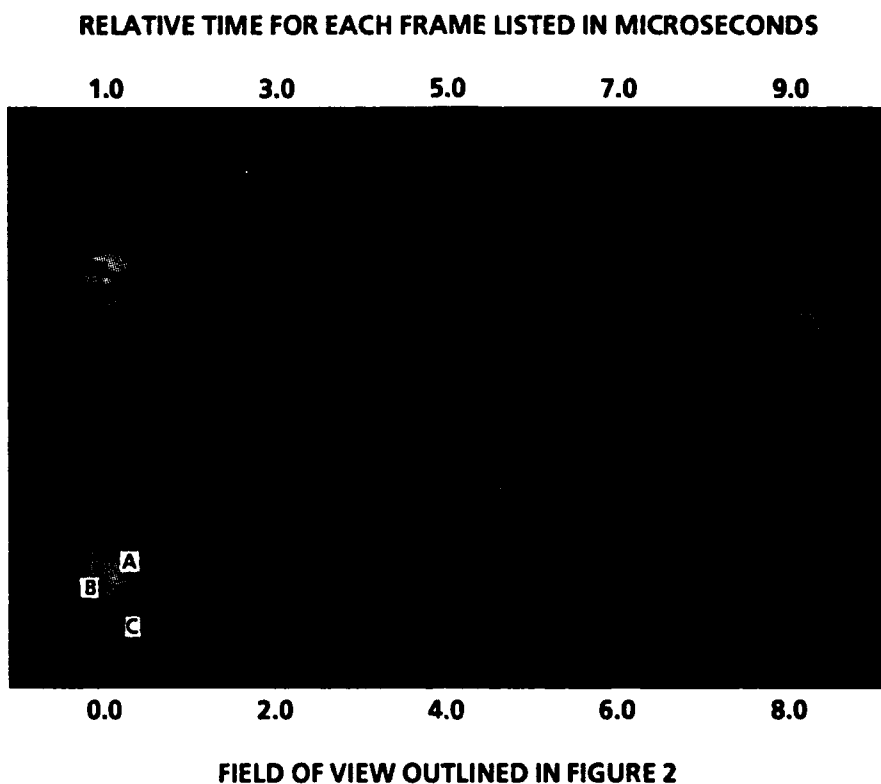


(B) CRYSTALLOGRAPHIC FEATURES, SHOTS ONR-29,30,31



(C) AFTER SHOCKED TO 38.5 KBAR, SHOT ONR-31

FIGURE 6. PHOTOMACROGRAPHS AND SCHEMATIC OF (001) SURFACE OF AP CRYSTALS AFTER SHOCK ENTRY INTO THAT SURFACE



DESCRIPTION OF EVENTS SEEN IN INDIVIDUAL FRAMES	
0.0 μ s	SHOCK ENTERED ($\bar{2}10$) SURFACE A. SHOCK FRONT B. CRYSTAL CORNER C. REFERENCE WIRES
1.0 μ s	SHOCK NEAR BOTTOM OF CRYSTAL; (010) AND ($\bar{1}00$) SLIP
2.0 μ s	SHOCK EXITED CRYSTAL; LUMINOSITY NEAR UPPER RIGHT CORNER
3.0 μ s - 9.0 μ s	LUMINOSITY FROM LIGHTLY DAMAGED AREAS NEAR TOP OF CRYSTAL

FIGURE 7. BACKLIT FRAMING CAMERA PHOTOGRAPHS OF (001) SURFACE OF AP CRYSTAL SHOCKED TO 24.4 KBAR, SHOT ONR-35

shocked portion of the crystal. Within that zone, there are dark diagonal lines that are associated with (010)[001] slip, which is the secondary deformation system impressions in the as-viewed (001) surface. Similar diagonal lines were more clearly shown in Figure 10 of Reference 1 for Shot ONR-19, which had a lower shock pressure of 16.7 kbar compared to 24.4 kbar in Shot ONR-35.

In the second frame (1.0 μ s), which was taken just as the shock approaches the bottom of the crystal, there is a relatively wide illuminated zone behind the shock front. This observation is similar to that for Shot ONR-18 (Figure 9 of Reference 1), which had the same P_{AP} but a narrower illuminated zone than in Shot ONR-35. Also in Shot ONR-18, the illuminated zone was brighter than the backlighting just below the crystal, indicating light from the chemical reaction of AP. The width of the illuminated zone behind the shock front in ONR-35 may be due partly to reaction light illuminating the crystal behind the shock front and partly to the increased separation of the shock fronts in the oil and the crystal. Because of the better focus on the film for the upper row of frames and the increased resolution of the film used in Shot ONR-35, the second frame reveals a number of features behind the shock front. As in the previous frame, there are dark diagonal lines behind the shock front that correspond to the volume-accommodating (010) slip deformation. One of these lines near the right of the frame is sufficiently broad to suggest that it is associated with a crack. However, the angle of this line relative to the [120] direction is too large to be a ($\bar{1}21$) crack as identified in Figure 8, which will be discussed later. Behind the shock front, there are small orthogonal crossing diagonal lines corresponding to both the ($\bar{1}00$) and (010) slip planes, which may not be visible in the photographic reproduction of Figure 7. These diagonal lines, which correspond to both the primary and secondary deformation systems, appear together on recovered crystals. However, ($\bar{1}00$) lines were not seen in the dynamic photographs of previous experiments.¹

By the third frame (2.0 μ s), the shock has just exited the bottom of the crystal, which is dark except for a small luminous region near the upper right corner. The size of this region expands in subsequent frames. Preexisting sources of light in the experiment can be reasonably eliminated as the cause of the luminous region. It is unlikely that hot gaseous detonator products were between the camera and the viewed (001) surface of the crystal because the luminous region is totally separated from the edge of the crystal in the 2.0 and 3.0 μ s frames. It is also unlikely that the luminosity was transmitted through the crystal from either backlighting or detonator products. The bottom region of the crystal (furthest from the detonator) remained dark in all of the frames after shock passage, even though this region of the recovered crystal was still optically transparent and was not visibly damaged (Figure 5(B)). In contrast, the mineral oil just under the crystal continued to transmit backlighting shortly after shock passage.

High-speed photographs of the ($\bar{2}10$) surface of crystals shocked through the (001) surface were obtained in Shots ONR-29,30,31. Neither microstructural features nor luminosity within the crystal was observed with shock passage. Following shock exit from the bottom surface of the crystal, there was a zone of luminosity below each crystal. In Shot ONR-30, this luminosity was only as intense as the backlighting. At the higher shock pressures in Shots ONR-29,31, the luminosity below the crystal was more intense, much like the detonator products above the crystal. When shock loading through the ($\bar{2}10$) surface, there was no luminosity observed below the crystal in Shot ONR-35 (Figure 7) and weak luminosity in Shot ONR-19 (Figure 10 of Reference 1).

MICROSTRUCTURAL CHARACTERIZATION OF RECOVERED CRYSTAL FROM SHOT ONR-35

Referring to the photomicrograph in Figure 8, numerous $(\bar{1}00)$ and (010) slip traces are readily apparent in the as-recovered (001) surface of the center-cleaved section of the AP crystal used in Shot ONR-35. These slip traces are finely spaced, sometimes appearing as shear bands, perhaps indicative of adiabatic heating. The $(\bar{1}00)$ traces significantly outnumber the (010) traces, as was observed previously in the recovered AP crystal in Shot ONR-19.¹ In addition to the slip trace formation, numerous $(\bar{1}21)$ cracks were found in the Shot ONR-35 crystal that were not observed in the Shot ONR-19 crystal. It is interesting to note that $(12\bar{1})$ cleavage steps were observed (Figure 3(B)) in the $(2\bar{1}0)$ surface of the AP crystal prior to shock loading in Shot ONR-35. It appears that there is some inherent weakness in the bonding across this plane that explains its propensity for cracking at high stress levels. It is possible that a dislocation reaction occurs, providing the nucleus for crack formation.

Low magnification SEM photographs of the right-hand cleaved section of the crystal (Figure 1) from Shot ONR-35 appear in Figure 9. The edge region formed by the intersection of the shock-entry $(2\bar{1}0)$ surface with Cleaved Plane #1 is shown in Figure 9(A). The major portion of the most prominent $(00\bar{1})$ crack branch that emanated from one corner of the Vickers hardness impression ($VHN = 9.1$) in the $(2\bar{1}0)$ surface is clearly visible. The crack surfaces have separated a distance of ~ 0.08 mm as a result of the cleaving operation since virtually no transverse separation in the crack branch was observed in light microscopy photographs of the hardness impression before or after the crystal was shock loaded. From these photographs, it was determined that the crack branch had undergone a very small radial extension of ≤ 0.03 mm as a result of shock loading. Also denoted in Figure 9(A) is a $(12\bar{1})$ crack, identified by performing a two-trace analysis on optical photographs of the crack intersecting the $(2\bar{1}0)$ and (001) surfaces. This observation connects directly with the $(12\bar{1})$ cleavage steps in Figure 3(B) and the $(\bar{1}21)$ cracks in Figure 8 discussed earlier.

The portion of Cleaved Plane #1 directly underneath the Vickers impression is shown in Figure 9(B). Considerable surface roughness is present indicating that $(2\bar{1}0)$ cleavage cracking did not occur easily. This is attributed to the hindering effect that work hardening, associated with forming the impression and/or shocking the crystal, has on crack propagation. The $(00\bar{1})$ crack branch present in Figure 9(A) is clearly visible in Figure 9(B), revealing now its depth of penetration into the crystal. The exact extent is obscured by surface roughness ~ 1.5 mm below the $(2\bar{1}0)$ surface. A fine $(00\bar{1})$ crack may actually extend ~ 2 mm below where the broad separation in the crack terminates (at ~ 1.25 mm from the shock-entry surface). The extent of the broadly separated crack was used in preparing the final figure (to be discussed later), which also shows the possible extension of the fine crack.

XPS ANALYSIS OF RECOVERED CRYSTAL FROM SHOT ONR-35

The results from analysis of the XPS spectra obtained across Cleaved Planes #1 and 2 (as denoted in Figure 1) are given in Figure 10. Approximate areas of analysis are outlined by the boxes superimposed on schematics of the cleaved planes, including locations of the Vickers hardness impressions. Appearing in the upper half of the boxes are values for %Cl as decomposition products, while values of the FWHM for the $Cl(2p_{3/2})$ peak are in the bottom half. Comparison with standards indicate that the decomposition product is a $Cl(+5)$ containing compound, most likely a

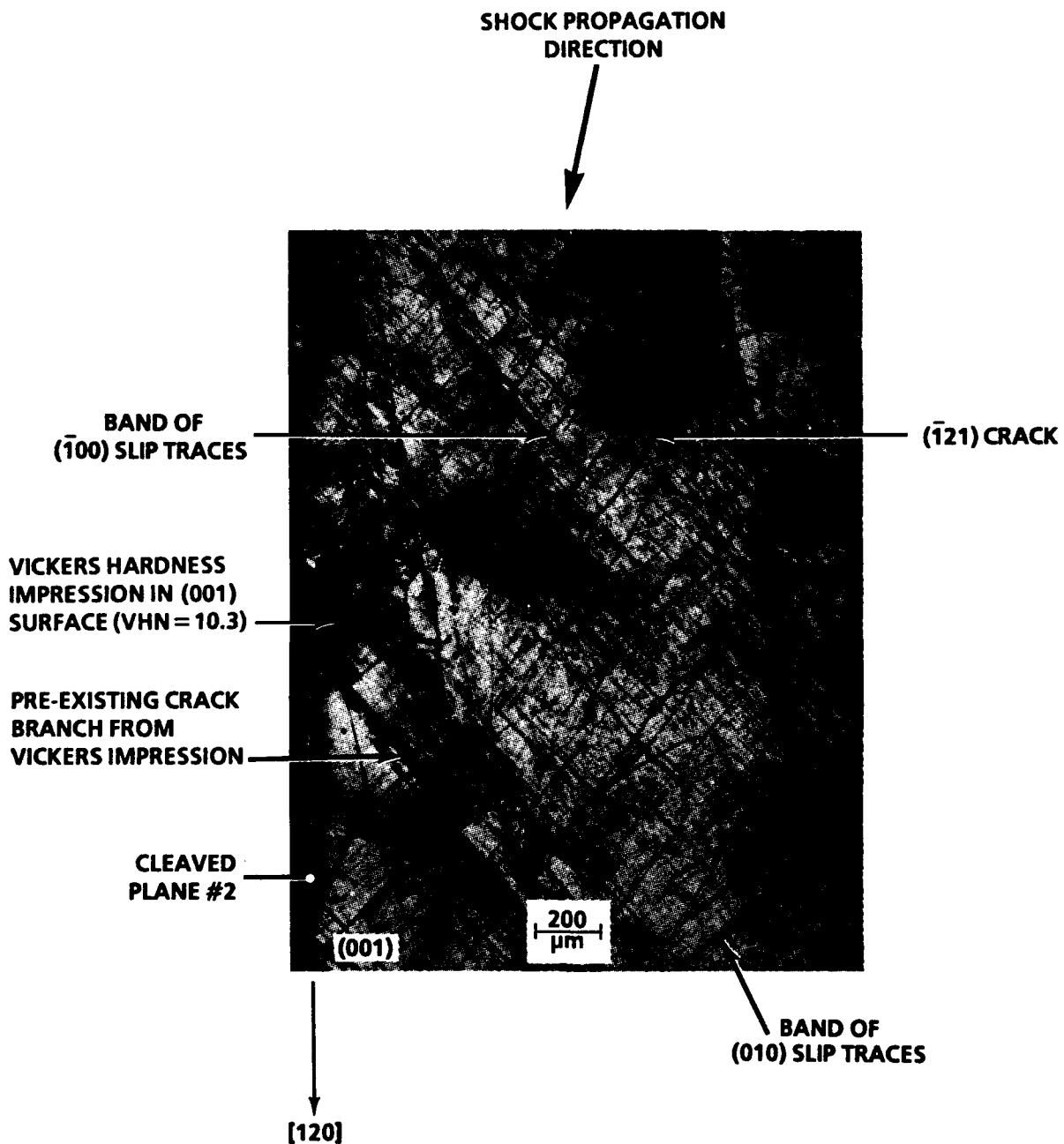


FIGURE 8. REFLECTED LIGHT PHOTOMICROGRAPH OF SLIP TRACES AND CRACKING NEAR CENTER OF EXTERIOR (001) SURFACE OF RECOVERED AP CRYSTAL, SHOT ONR-35

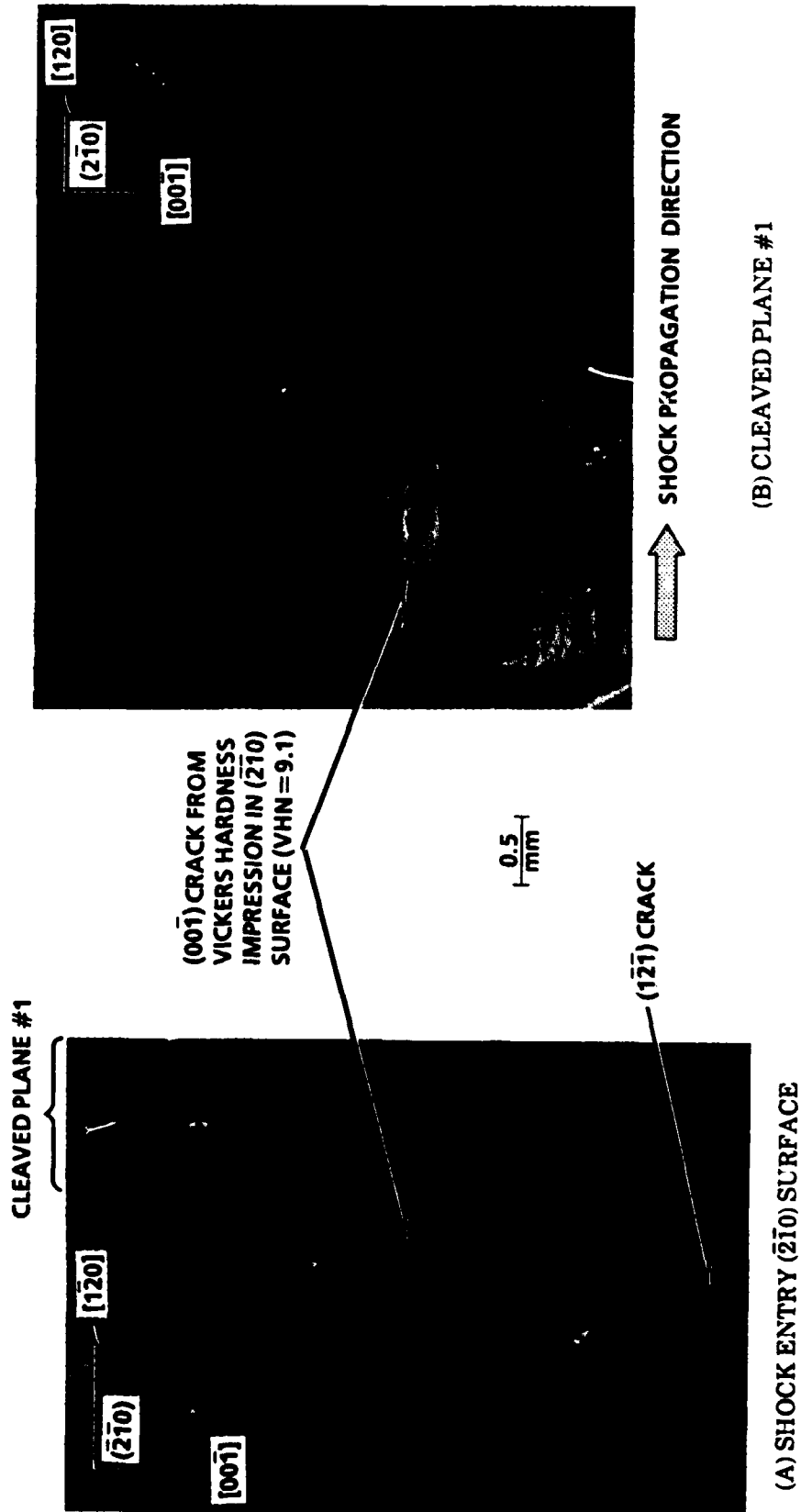
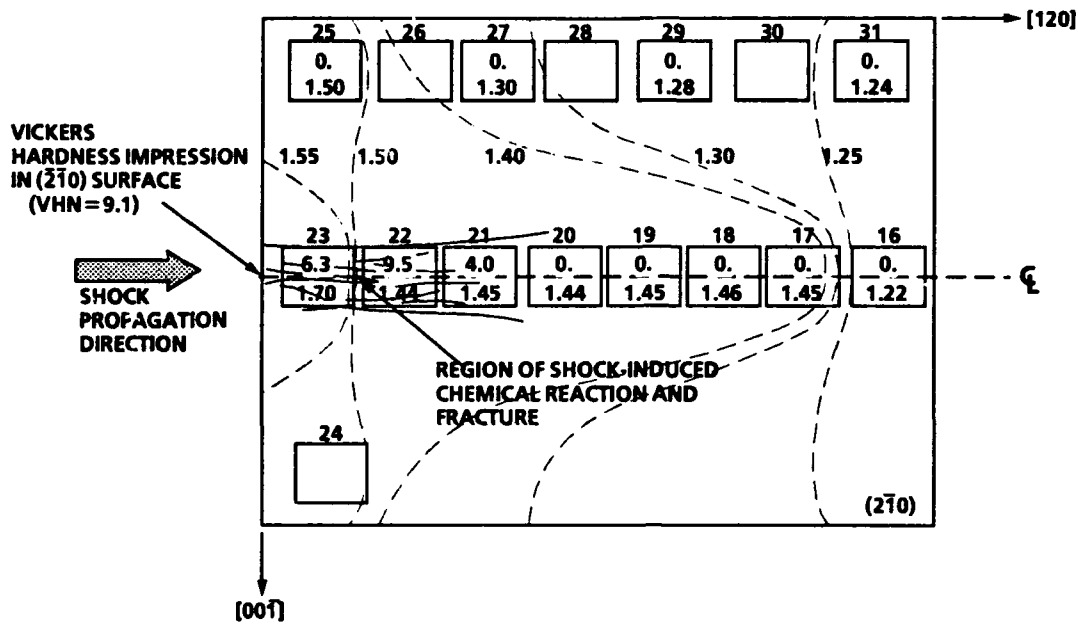


FIGURE 9. LOW MAGNIFICATION SEM PHOTOGRAPHS OF CRACKING IN VICINITY OF $(\bar{2}\bar{1}0)$ VICKERS HARDNESS IMPRESSION IN RECOVERED AP CRYSTAL, SHOT ONR-35

BOXES INDICATE 1 mm² XPS ANALYSIS AREA

25

XPS RUN NUMBER

0.
1.50

%Cl AS DECOMPOSITION PRODUCTS

FWHM Cl (2p, 3/2) PEAK

FWHM = FULL WIDTH OF PEAK AT HALF MAXIMUM HEIGHT

CONTOUR LINES CONNECT FWHM REGIONS OF SIMILAR VALUE

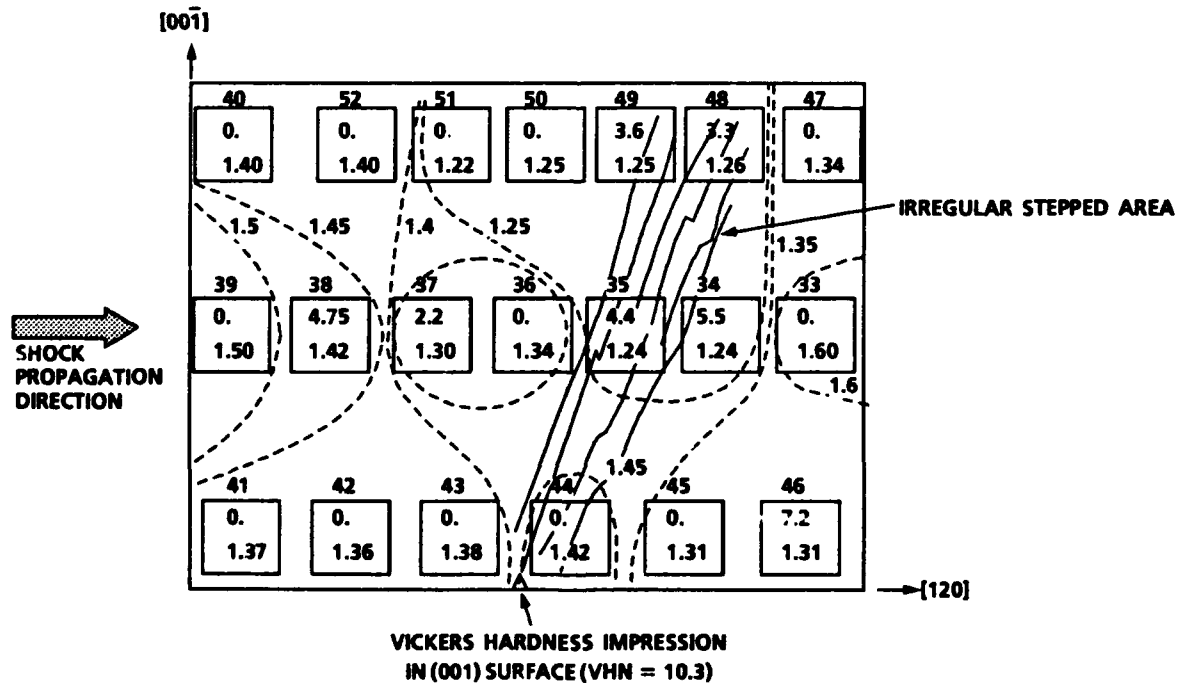
1.0
mm

FIGURE 10. XPS ANALYSIS RESULTS FROM INTERIOR OF AP CRYSTAL SHOCKED TO 24.4 KBAR, SHOT ONR-35

chlorate salt. The run numbers, indicating the order of the analyses, appear at the top of the boxes. Cl(2p) spectra from Runs #16 and 25 on Cleaved Plane #1 (Figure 10(A)) appear in Figure 4 of Reference 6. Emphasis was given to following the chlorine spectra since the nitrogen spectra from the same analysis areas showed no indication of chemical change.

Referring to Figure 10(A), spot analyses were performed along the centerline and one edge of Cleaved Plane #1. Spectra were not collected along the opposite edge because excessive charging made the data useless. Contour lines connect regions of equivalent FWHM of the Cl(2p, 3/2) peak. A mirror image was projected across the centerline to provide symmetrical data points along the edge not analyzed. The highest levels of shock-induced line broadening occurred immediately below the shock-entry surface, where the largest increase was detected in the vicinity of the Vickers hardness impression (VHN = 9.1). Elevated FWHM values of ~1.45 persisted along the centerline for nearly the entire length of the crystal. The bottom centerline FWHM value of 1.22 is identical to the value obtained in an unshocked AP crystal (control).⁶

The yields of %Cl as decomposition products measured on Cleaved Plane #1 do not correspond spatially one-to-one with the increased line broadening values. Chemical changes are limited to the centerline area directly underneath the hardness impression and occur for ~3.5 mm in the [120] direction. This area encompasses the (00 $\bar{1}$) crack appearing in Figure 9(B) and its strain field. The highest decomposition level (9.5 percent chlorine in the (+5) state) was found at the termination of the broad separation in the crack. In centerline regions below this, with essentially the same ~1.45 FWHM value, there was no detected chemical decomposition. This was also the case for the corner region near the shock-entry surface having a 1.50 FWHM value.

In Figure 10(B), the spot analyses for Cleaved Plane #2 show that the chemical changes and line broadening followed a different spatial distribution. In contrast to Cleaved Plane #1, there was no chemical change detected in the vicinity of the hardness impression or immediately below the shock-entry surface. However, there were significant changes measured further below that surface that correspond in location to results obtained for Cleaved Plane #1. Significant chemical changes also occurred toward the bottom along the center and near the edge opposite the indented surface. These changes were in a region where a series of irregular cleavage steps were observed to emanate from the hardness impression. The largest line broadening measurement was obtained in the center bottom region but is probably anomalous because it does not correlate with the visible appearance or the dislocation etch pit count. Otherwise, the region just underneath the shock-entry surface exhibited the greatest line broadening, as was the case for Cleaved Plane #1. Significant line broadening also occurred in the proximity of the Vickers hardness impression (VHN = 10.3) put into the (001) surface.

ADDITIONAL XPS RESULTS

Chlorate concentrations of 3.5 to 4.7 atom percent were observed at the mid-plane parallel to the shock-entry surface of the crystal recovered from Shot ONR-24. At comparable locations in ONR-35 no chlorate was observed. Analysis of the {210} surface intersecting the shock-entry surface revealed the parent perchlorate, Cl(+7), and chlorate, Cl(+5), as noted before. There was also a new component in the Cl(2p) spectra having a binding energy intermediate to that for chloride, Cl(-1), and

chlorite, $\text{Cl} (+3)$. A $\text{Cl} (+1)$ state is therefore strongly suggested by the observation of this peak. Concentrations of this new component ranged from 4.2 to 5.4 atom percent. This chemical state was not observed at the lower shock pressure in Shot ONR-35. Drop-weight impact data have found concentrations of up to 20 atom percent in this chemical state in the absence of any increased concentration of the chlorate.¹¹ This suggests that the $\text{Cl} (+1)$ is a more highly reacted product, whereas the chlorate participates as a reactive intermediate.

In both Shots ONR-24 and 35, there was no observed change in the nitrogen chemistry. Thus, the chemistry induced by shock passage appears to produce reduced oxychloride anions as stable intermediate decomposition products. Production of oxidized nitrogen (i.e., NO , NO_2) or O_2 is likely, but none of these are detectable since the spectrometer used can only analyze solid materials.

DISCUSSION

It is speculated for Shot ONR-35 that the luminosity from shock loading the crystal, which first appears in the 2.0 μs frame in Figure 7, was caused by chemical reaction occurring in the strain field of the Vickers hardness impression put into the shock-entry ($\bar{2}10$) surface. A schematic in Figure 11 of the crystal, as viewed by the camera, shows the region of luminosity along with various other features, including the large $(00\bar{1})$ crack under the impression on the shock-entry surface. Luminosity could not be observed directly in the vicinity of the $(00\bar{1})$ crack because of the extensive damage in this region of the crystal, as indicated by the in-depth cloudiness in the recovered crystal (Figure 5(B)). Rather, the luminosity was observed from near the boundary of the most damaged regions of the crystal. This in-depth boundary between the cloudy and clear regions of the recovered crystal is delineated by a short-dashed line in Figure 11 and passes through the region of luminosity observed in the 3.0 μs frame.

The pattern of light from the crystal in the Figure 7 high-speed photographs after the 3.0 μs frame coincides with the in-depth boundary for crystal damage in Figure 11. This indicates that the damage observed in the recovered crystal occurred sometime during the shock process (i.e., loading and subsequent unloading) rather than from capturing the crystal in the foam catcher (Figure 2). The degree of curvature observed for the propagating shock in the 0.0 and 1.0 μs frames in Figure 7 is less than that for the in-depth boundary of crystal damage appearing in Figures 5(B) and 11. The increased curvature for the damage boundary is attributed to lateral rarefactions which reduce the shock intensity and duration. Thus, a threshold condition for shock/rarefaction interplay was present to cause visible damage (cloudiness). The in-depth boundary for crystal damage is uniformly curved except in the vicinity of the two hardness impressions on the (001) surface. This boundary is extended further from the shock-entry surface for the left impression ($\text{VHN} = 10.3$), whereas cloudiness is greatly reduced in the vicinity of the right impression ($\text{VHN} = 10.5$). The right impression is near the impression in the shock-entry ($\bar{2}10$) surface. This suggests that the large $(00\bar{1})$ crack (Figures 9 and 11) associated with the latter impression reduces damage by allowing shock-generated dislocations to escape.

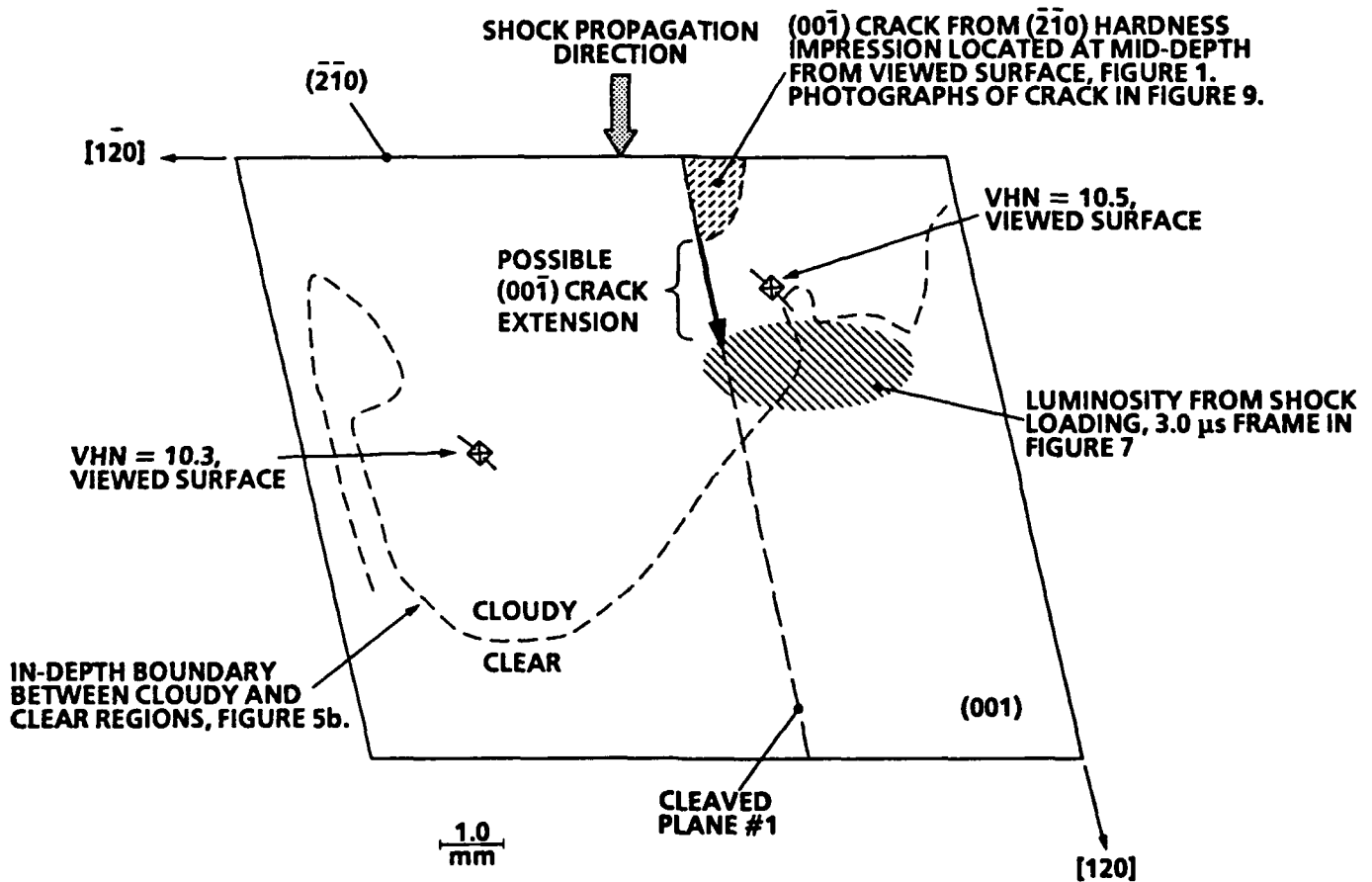


FIGURE 11. SCHEMATIC OF VARIOUS FEATURES VIEWED ON OR THROUGH (001) SURFACE OF RECOVERED AP CRYSTAL, SHOT ONR-35

Unfortunately, there was not sufficient time resolution in the high-speed photographs to distinguish unequivocally the roles of shock loading and unloading on microstructural changes and consequent enhanced chemical reactivity. The photographs for Shot ONR-19 (Figure 10 in Reference 1), in particular, clearly show slip traces joining the shock front, suggesting that the loading process is responsible for the damage observed in recovered crystals (e.g., Figures 11 to 13 in Reference 1 and Figure 5(B)). However, luminosity attributed to crack propagation (Figure 9 in Reference 1) or occurring in the vicinity of the Vickers impressions (Figure 9 in Reference 1 and Figure 7) has always been observed to occur one or more microseconds after shock passage. This indicates either that the unloading process influences shock reactivity or that there is an induction time before the onset of reaction.

Some of the slip systems involved in accommodating the Vickers indenter at low strain rate were also active in the shocked crystals. In particular, the numerous diagonal lines appearing in some high-speed photographic frames were attributed to two prominent slip systems identified from hardness testing: (010)[001] and (100)[001]. The resultant slip traces were readily seen in the external (001) surface of the recovered crystal (Figure 8). Several crack planes, namely ($\bar{2}$ 10), (110), (230), and ($\bar{1}$ 21), occurring in shocked crystals were not involved in forming the indentations. Although ($\bar{2}$ 10) cleavage cracking has been observed by other researchers,¹²⁻¹⁴ the remaining planes have not been reported previously. The occurrence of these crack planes indicates that shocking provided higher stresses normal to these planes than what were present during hardness testing.

The combined XPS results for Cleaved Planes #1 and 2 indicate that the largest amounts of chemical decomposition were associated with the Vickers hardness impressions put into the crystal prior to shock loading. However from Figure 10(B), the character of the shock (pressure and duration) was sufficient in Shot ONR-35 to cause decomposition along the centerline away from the influence of the impression. This provides a confirmation of the previous LIC determination of reaction threshold to be $P_{AP} \sim 24.4$ kbar when hardness impressions in the crystal are absent (Shot ONR-17).¹

Line broadening of the XPS spectra from Cleaved Planes #1 and 2 was enhanced in the vicinity of the impressions, particularly for the impression in the ($\bar{2}$ 10) shock-entry surface. This resulted from the interaction of the shock with the dislocations and their cumulative strain fields associated with the impressions. By comparison, no increased broadening of XPS spectra was detected near the impression in an unshocked AP crystal (control) which was freshly cleaved to provide a replica of Cleaved Plane #1.

Variation in line broadening measurements has been related to the shock damage appearing in Figure 5(B). The visual damage was compared⁶ previously to that in AP crystals irradiated by Herley and Levy,^{15,16} who correlated the degree of cloudiness with dislocation densities measured in a chemical etch pitting study. It was estimated that an $\sim 100X$ increase in dislocation density exists from the bottom of the crystal to the shock-entry surface.⁶ In subsequent work, another freshly cleaved surface approximately centered between Cleaved Planes #1 and 2 was chemically etched, and dislocation density measurements were obtained. An $\sim 100X$ increase in dislocation density in the region of the crystal immediately below the shock-entry ($\bar{2}$ 10) surface was also obtained by extrapolation of dislocation density measurements correlated spatially to XPS line-width measurements.⁷ Molecular orbital energy

level calculations confirmed the effect of lattice disruption on increased XPS line width.^{6,7}

The molecular nature of the species observed with XPS has been investigated to explore more fully the solid-state decomposition chemistry of AP. Secondary ion mass spectrometry was employed for analyzing products in impacted and irradiated samples of AP. Relative to a control sample from a freshly cleaved AP single crystal, these damaged samples displayed mass-to-charge ratio (m/e) peaks which have been tentatively attributed to HClO_3 ($m/e = 90$, $\text{Cl}(+5)$); NHCl_2 ($m/e = 85$, $\text{Cl}(+1)$); and NH_2Cl ($m/e = 51$, $\text{Cl}(+1)$). These molecular species are, therefore, proposed as the source of XPS signals appearing at the $\text{Cl}(+5)$ and $\text{Cl}(+1)$ chemical states in the current work.

SUMMARY AND CONCLUSIONS

Additional results, to relate to earlier work, have been obtained for the roles that deformation, fracture, and material microstructure have on the shock reactivity of AP. Emphasis was given to a detailed analysis of one experiment in which a large crystal, containing several Vickers hardness impressions, was subjected to a shock at the reaction threshold, ~ 25 kbar. The crystal was recovered intact. Microstructural characterization was conducted using light and scanning electron microscopies. X-ray photoelectron spectroscopy was used to scan $1\text{ mm} \times 1\text{ mm}$ areas across two freshly cleaved surfaces that cut right through the hardness impressions. The most significant finding was that the largest amounts of chemical decomposition occurred because of the presence of the impressions. For the impression put into the shock-entry ($2\bar{1}0$) surface, decomposition was detected directly underneath over a depth of 3.5 mm. This decomposition seemed to be associated with a large ($00\bar{1}$) crack, that formed at the impression prior to shock loading and possibly had penetrated to that distance. For an impression put into the (001) surface, no evidence of decomposition was found in close proximity. Rather, decomposition was detected in an area of irregular cleavage steps that emanated from the impression and extended the entire depth of the crystal, ~ 7 mm. A series of high-speed photographs taken during shock loading of the crystal revealed an enlarging, elliptically-shaped luminous zone located off center from, but encompassing, the furthest possible extension of the ($00\bar{1}$) crack. The combined observations indicate that the luminosity resulted from chemical reaction occurring either at the tip of the ($00\bar{1}$) crack or in its plastic zone.

REFERENCES

1. Sandusky, H.W., Glancy, B.C., Carlson, D.W., Elban, W.L., and Armstrong, R.W., "Relating Deformation to Hot Spots in Shock-Loaded Crystals of Ammonium Perchlorate," *Journal of Propulsion and Power*, Vol. 7, No. 4, 1991, pp. 518-525.
2. Elban, W.L., Coyne, P.J., Jr., Sandusky, H.W., Glancy, B.C., Carlson, D.W., and Armstrong, R.W., *Investigation of the Origin of Hot Spots in Deformed Crystals: Studies on Ammonium Perchlorate and Reference Inert Materials*, NSWC MP 88-178, Apr 1988, Naval Surface Warfare Center, Silver Spring, MD.
3. Elban, W.L., and Armstrong, R.W., "Plastic Anisotropy and Cracking at Hardness Indentations in Single Crystal Ammonium Perchlorate," to be submitted to *Journal of Materials Science*.
4. Thomas, J.M., "Enhanced Reactivity at Dislocations in Solids," in *Advances in Catalysis and Related Subjects*, Eds.: Eley, D.D., Pines, H., and Weisz, P.B., Academic Press, New York, NY and London, UK, 1969, pp. 293-400.
5. Thomas, J.M., "The Chemistry of Deformed and Imperfect Crystals," *Endeavour*, Vol. 29, No. 108, 1970, pp. 149-155.
6. Beard, B.C., Sharma, J., Sandusky, H.W., Glancy, B.C., and Elban, W.L., "Dislocation Density Variation in Shocked Single Crystal Ammonium Perchlorate," in *Shock Compression of Condensed Matter - 1991*, Eds., Schmidt, S. C., Dick, R. D., Forbes, J. W., and Tasker, D. G., North-Holland, Amsterdam, 1992, pp. 571-574.
7. Beard, B.C., Sandusky, H.W., Glancy, B.C., and Elban, W.L., "Defect Density Measurements in Shocked Single Crystal Ammonium Perchlorate by X-Ray Photoelectron Spectroscopy," *Journal of Materials Research*, Vol. 7, No. 12, 1992, pp. 3266-3274.
8. Frank, F.C., and Lawn, B.R., "On the Theory of Hertzian Fracture," *Proceedings of the Royal Society of London*, Ser. A, Vol. 299, No. 1458, 1967, pp. 291-306.
9. Lawn, B.R., and Fuller, E.R., "Equilibrium Penny-like Cracks in Indentation Fracture," *Journal of Materials Science*, Vol. 10, No. 12, 1975, pp. 2016-2024.

REFERENCES (Continued)

10. Armstrong, R.W., and Elban, W.L., "Cracking at Hardness Micro-indentations in RDX Explosive and MgO Single Crystals," *Materials Science and Engineering*, Vol. A111, 1989, pp. 35-43.
11. Sharma, J., Hoffsommer, J.C., Glover, D.J., Coffey, C.S., Forbes, J.W., Liddiard, T.P., Elban, W.L., and Santiago, F., "Sub-ignition Reactions at Molecular Levels in Explosives Subjected to Impact and Underwater Shock," in *Proceedings Eighth Symposium (International) on Detonation*, 15-19 Jul 1985, NSWC MP 86-194, Naval Surface Warfare Center, Silver Spring, MD, pp. 725-733.
12. Tutton, A.E.H., "The Alkali Perchlorates and a New Principle Concerning the Measurement of Space-lattice Cells," *Proceedings of the Royal Society of London*, Ser. A., Vol. 111, No. 759, 1926, pp. 462-491.
13. Herley, P.J., Jacobs, P.W.M., and Levy, P.W., "Dislocations in Ammonium Perchlorate," *Journal of the Chemical Society*, Section A, No. 3, 1971, pp. 434-440.
14. Williams, J.O., Thomas, J.M., Savintsev, Y.P., and Boldyrev, V.V., "Dislocations in Orthorhombic Ammonium Perchlorate," *Journal of the Chemical Society*, Section A, No. 11, 1971, pp. 1757-1760.
15. Herley, P.J., and Levy, P.W., "Quantitative Studies of Radiation Induced Dislocations and the Decomposition Kinetics of Ammonium Perchlorate," in *Proceedings 7th International Symposium on the Reactivity of Solids*, 17-21 Jul 1972, Chapman and Hall, London, UK, pp. 387-395.
16. Herley, P.J., and Levy, P.W., "Microscopic Observation of X-ray and Gamma-ray Induced Decomposition of Ammonium Perchlorate Crystals," in *Proceedings of American Nuclear Society AIAA Conference on Natural and Man-made Radiation in Space*, NASA Technical Memorandum X-2440, 1972, pp. 584-592.

DISTRIBUTION

	<u>Copies</u>		<u>Copies</u>
ATTN AIR 320 G	1	ATTN ADMINISTRATION	
AIR 320 R	1	CONTRACTING	
COMMANDER		OFFICER (M T MCCracken)	1
NAVAL AIR SYSTEMS COMMAND		OFFICE OF NAVAL RESEARCH	
DEPARTMENT OF THE NAVY		NATIONAL ACADEMY OF SCIENCES	
WASHINGTON DC 20361		2135 WISCONSIN AVE NW	
		ROOM 102	
ATTN SEA 06AFR (R MUIR)	1	WASHINGTON DC 20007-2259	
SEA 662 (R BOWEN)	1		
COMMANDER		ATTN ONT 20T (P QUINN)	1
NAVAL SEA SYSTEMS COMMAND		ONT 21 (DR E ZIMET)	1
DEPARTMENT OF THE NAVY		ONT 23 (DR A FAULSTICH)	1
WASHINGTON DC 20362-5105		ONT 232 (D HOUSER)	1
		OFFICE OF NAVAL TECHNOLOGY	
ATTN SP 2731 (E THROCKMORTON)	1	DEPARTMENT OF THE NAVY	
DIRECTOR		800 NORTH QUINCY STREET	
STRATEGIC SYSTEMS PROGRAMS		ARLINGTON VA 22217-5660	
DEPARTMENT OF THE NAVY			
WASHINGTON DC 20376-5002		ATTN CODE 2627 (DIRECTOR)	1
		CODE 6120 (DR W MONIZ)	1
ATTN CODE 5253	1	CODE 6120 (DR D PACE)	1
CODE 5253 (J BIRKETT)	1	CODE 6360 (DR C CM WU)	1
COMMANDER		CODE 6540 (DR W FAUST)	1
INDIAN HEAD DIVISION		COMMANDING OFFICER	
NAVAL SURFACE WARFARE CENTER		NAVAL RESEARCH LABORATORY	
INDIAN HEAD MD 20640-5000		4555 OVERLOOK AVE SW	
		WASHINGTON DC 20375-5000	
ATTN NEDED	1		
OFFICER IN CHARGE		ATTN CODE 38 (DR R DERR)	1
INDIAN HEAD DIVISION		CODE 3205 (DR F MARKARIAN)	1
NAVAL SURFACE WARFARE CENTER		CODE 385 (DR R HOLLINS)	1
YORKTOWN DETACHMENT		CODE 38503 (DR A NEILSON)	1
YORKTOWN VA 23692-5110		CODE 3853 (DR R YEE)	1
		CODE 389 (T BOGGS)	1
ATTN CODE 1132P (DR R MILLER)	5	CODE 3891 (A ATWOOD)	1
CODE 1112AI		CODE 3891 (M CHAN)	1
(DR D LIEBENBERG)	1	CODE 3891 (H RICHTER)	1
OFFICE OF NAVAL RESEARCH		CODE 3892 (DR T PARR)	1
DEPARTMENT OF THE NAVY		COMMANDER	
800 NORTH QUINCY STREET		NAVAL AIR WARFARE CENTER	
ARLINGTON VA 22217-5660		CHINA LAKE CA 93555-6001	

DISTRIBUTION (Continued)

	<u>Copies</u>		<u>Copies</u>
ATTN CODE 5063 (DR H WEBSTER III)	1	ATTN DR D BALL	1
COMMANDER		DR A MATUSZKO	1
NAVAL WEAPONS SUPPORT CENTER		AIR FORCE OFFICE OF SCIENTIFIC	
MANAGER CHEMICAL SCIENCES		RESEARCH	
BRANCH		BOLLING AIR FORCE BASE	
CRANE IN 47522		WASHINGTON DC 20332	
ATTN CODE RD 1 (DR A SLAFKOSKY)	1	ATTN G PARSONS	1
COMMANDANT OF THE MARINE CORPS		DR R MCKENNEY	1
SCIENTIFIC ADVISOR		J CORLEY	1
WASHINGTON DC 20380		LIBRARY	1
ATTN SMCAR AEE (DR J LANNON)	1	DEPARTMENT OF THE AIR FORCE	
SMCAR AEE WW		WL MNME	
(DR D WIEGAND)	1	EGLIN AFB FL 32542-5434	
COMMANDER		ATTN DY/MS 24 (R GEISLER)	1
US ARMY ARDEC		AFRPL	
PICATINNY ARSENAL NJ 07806-5000		EDWARDS AFB CA 93523	
ATTN SLCBR IB I (DR A MIZIOLEK)	1	ATTN DR J WILKES JR	1
SLCBR IB P (J ROCCHIO)	1	NJSRL/NC	
SLCBR TB EE (DR R FREY)	1	USAF ACADEMY CO 80840	
ARMY BALLISTIC RESEARCH		ATTN DR J GILMAN	1
LABORATORIES		LAWRENCE BERKELEY NATIONAL	
ABERDEEN PROVING GROUND		LABORATORY	
MD 21005-5066		UNIVERSITY OF CALIFORNIA	
ATTN DRSMI RKL (DR W WHARTON)	1	BUILDING 50B-3238	
COMMANDER		BERKELEY CA 94720	
US ARMY MISSILE COMMAND		ATTN CODE L 282 (DR R SIMPSON)	1
REDSTONE ARSENAL AL 35898		CODE L 282 (DR W TAO)	1
ATTN CHEMICAL & BIOLOGICAL		CODE L 369	
SCIENCES DIVISION	1	(DR M COSTANTINO)	1
ENGINEERING DIV (DR D MANN)	1	LAWRENCE LIVERMORE NATIONAL	
US ARMY RESEARCH OFFICE		LABORATORY	
BOX 12211		UNIVERSITY OF CALIFORNIA	
RESEARCH TRIANGLE PARK		PO BOX 808	
NC 27709-2211		LIVERMORE CA 94551-0808	
ATTN DR D SAYLES	1	CENTER FOR NAVAL ANALYSES	
BALLISTIC MISSILE DEFENSE		4401 FORD AVENUE	
ADVANCED TECHNOLOGY CENTER		ALEXANDRIA VA 22302-0268	1
PO BOX 1500			
HUNTSVILLE AL 35807			

DISTRIBUTION (Continued)

	<u>Copies</u>		<u>Copies</u>
ATTN DR H CADY	1	ATTN G ZIMMERMAN	1
J DALLMAN	1	AEROJET TACTICAL SYSTEMS	
DR J DICK	1	PO BOX 13400	
DR J DIENES	1	SACRAMENTO CA 95813	
DR J RAMSAY	1		
DR J RITCHIE	1	ATTN DR M KING	1
DR C STORM	1	ATLANTIC RESEARCH CORP	
DIRECTOR		5390 CHEROKEE AVENUE	
LOS ALAMOS NATIONAL LABORATORY		ALEXANDRIA VA 22312	
LOS ALAMOS NM 87545			
		ATTN M BARNES	1
ATTN DR R BEHRENS	1	G BOWMAN	1
DR C MELIUS	1	R SHENTON	1
SANDIA NATIONAL LABORATORIES		W WAESCHE	1
PO BOX 969		B WHEATLEY	1
LIVERMORE CA 94551-0969		ATLANTIC RESEARCH CORP	
		7511 WELLINGTON ROAD	
ATTN DR R GRAHAM	1	GAINESVILLE VA 22065	
SANDIA NATIONAL LABORATORIES			
PO BOX 5800		ATTN DR C FREY	1
ALBUQUERQUE NM 87185-5800		CHEMICAL SYSTEMS DIVISION	
		PO BOX 358	
ATTN G74 (TA)	1	SUNNYVALE CA 94086	
NSACSS			
FT GEORGE G MEADE MD 20755		ATTN DR E DEBUTTS	1
		HERCULES AEROSPACE CO	
ATTN CPIA	1	PO BOX 27408	
THE JOHNS HOPKINS UNIVERSITY		SALT LAKE CITY UT 84127	
10630 LITTLE PATUXENT PARKWAY			
SUITE 202		ATTN DR K HARTMAN	1
COLUMBIA MD 21044-3200		HERCULES INCORPORATED	
		HERCULES AEROSPACE DIV	
ATTN GIFT AND EXCHANGE DIV	4	PO BOX 210	
LIBRARY OF CONGRESS		CUMBERLAND MD 21502	
WASHINGTON DC 20540			
DEFENSE TECHNICAL INFORMATION		ATTN G BUTCHER	1
CENTER		HERCULES INCORPORATED	
CAMERON STATION		MS X2H	
ALEXANDRIA VA 22304-6145	12	PO BOX 98	
		MAGNA UT 84044	
ATTN DR R LOU	1		
DR R OLSEN	1	ATTN DR R MARTINSON	1
DR R PETERS	1	LOCKHEED MISSILES & SPACE CO	
DR R STEEL	1	RESEARCH AND DEVELOPMENT	
AEROJET STRATEGIC PROPULSION CO		3251 HANOVER STREET	
PO BOX 15699C		PALO ALTO CA 94304	
SACRAMENTO CA 95813			

DISTRIBUTION (Continued)

	<u>Copies</u>		<u>Copies</u>
ATTN G LO	1	ATTN DR D CURRAN	1
LOCKHEED PALO ALTO RESEARCH		DR D MCMILLEN	1
LABORATORY		DR J ROSENBERG	1
B204		DR D SHOCKLEY	1
PALO ALTO CA 94304		SRI INTERNATIONAL	
		333 RAVENSWOOD AVENUE	
ATTN DR R KRUSE	1	MENLO PARK CA 94025	
MORTON THIOKOL INC			
HUNTSVILLE DIVISION		ATTN DR R VALENTINI	1
HUNTSVILLE AL 35807-7501		UNITED TECHNOLOGIES CHEMICAL	
		SYSTEMS	
ATTN T DAVIDSON	1	PO BOX 50015	
D FLANIGAN	1	SAN JOSE CA 95150-0015	
MORTON THIOKOL INC			
AEROSPACE GROUP		ATTN PROF A GENT	1
110 NORTH WACKER DRIVE		UNIVERSITY OF AKRON	
CHICAGO IL 60606		INSTITUTE OF POLYMER SCIENCE	
		AKRON OH 44325	
ATTN L ESTABROOK	1		
DR J WEST	1	ATTN PROF M NICOL	1
MORTON THIOKOL INC		UNIVERSITY OF CALIFORNIA	
PO BOX 30058		DEPT OF CHEMISTRY AND	
SHREVEPORT LA 71130		BIOCHEMISTRY	
		405 HILGARD AVENUE	
ATTN S PALOPOLI	1	LOS ANGELES CA 90024	
MORTON THIOKOL INC			
ELKTON DIVISION		ATTN PROF T BRILL	1
PO BOX 241		UNIVERSITY OF DELAWARE	
ELKTON MD 21921		DEPARTMENT OF CHEMISTRY	
		NEWARK DE 19716	
ATTN DR D DILLEHAY	1		
MORTON THIOKOL INC		ATTN PROF E PRICE	1
LONGHORN DIVISION		GEORGIA INSTITUTE OF TECHNOLOGY	
MARSHALL TX 75760		SCHOOL OF AEROSPACE ENGINEERING	
		ATLANTA GA 30332	
ATTN J HINSHAW	1		
G THOMPSON	1	ATTN PROF W ELBAN	25
MORTON THIOKOL INC		DEAN D ROSWELL	1
WASATCH DIVISION		MR T SCHEYE	1
PO BOX 524		LOYOLA COLLEGE	
BRIGHAM CITY UT 84302		4501 N CHARLES STREET	
		BALTIMORE MD 21210-2699	
ATTN DR M FARBER	1		
SPACE SCIENCES INC			
135 MAPLE AVENUE			
MONROVIA CA 91016			

DISTRIBUTION (Continued)

	<u>Copies</u>		<u>Copies</u>
ATTN PROF H AMMON	1	INTERNAL DISTRIBUTION	
PROF R ARMSTRONG	5	C831 D CARLSON	1
DR X ZHANG	1	E35	1
UNIVERSITY OF MARYLAND		E231	2
COLLEGE PARK MD 20742		E232	3
		R	1
ATTN CODE 012(DR J WALL)	1	R10	1
NAVAL POSTGRADUATE SCHOOL		R101	1
DIRECTOR		R10A	1
RESEARCH ADMINISTRATION		R10A2	1
MONTEREY CA 93943		R10B	1
		R11	1
ATTN DR K BROWER	1	R11 M CHAYKOVSKY	1
PROF P A PERSSON	1	R11 S DEITER	1
NEW MEXICO INSTITUTE OF MINING		R11 C GOTZMER	1
& TECHNOLOGY		R11 L JOHNSON	1
SOCORRO NM 87801		R11 J LEAHY	1
		R11 T RUSSELL	1
ATTN PROF P POLITZER	1	R11 M SITZMANN	1
UNIVERSITY OF NEW ORLEANS		R11 S TURNER	1
DEPARTMENT OF CHEMISTRY		R11 G WILMOT	1
NEW ORLEANS LA 70148		R12	1
		R12 B GLANCY	5
ATTN PROF K KUO	1	R13	1
PENNSYLVANIA STATE UNIVERSITY		R13 R BERNECKER	1
DEPT OF MECHANICAL ENGINEERING		R13 C COFFEY	1
UNIVERSITY PARK PA 16802		R13 J DAVIS	1
		R13 J FORBES	1
ATTN PROF A DE LOZANNE	1	R13 P GUSTAVSON	1
PROF R SCHAPERY	1	R13 S JACOBS	1
UNIVERSITY OF TEXAS		R13 H JONES	1
AUSTIN TX 78712		R13 E LEMAR	1
		R13 P MILLER	1
ATTN PROF J DICKINSON	1	R13 DTASKER	1
PROF Y GUPTA	1	R13 H SANDUSKY	10
PROF M MILES	1	R13 G SUTHERLAND	1
WASHINGTON STATE UNIVERSITY		R13 W WILSON	1
DEPARTMENT OF PHYSICS		R13 D WOODY	1
PULLMAN WA 99163		R14	1
		R15	1
ATTN PROF M MCBRIDE	1	R34 M NORR	1
YALE UNIVERSITY		R34 J SHARMA	1
DEPARTMENT OF CHEMISTRY			
PO BOX 6666			
NEW HAVEN CT 06511			

REPORT DOCUMENTATION PAGE

Form Approved
OMB No. 0704-0188

Public reporting burden for this collection of information is estimated to average 1 hour per response, including the time for reviewing instructions, searching existing data sources, gathering and maintaining the data needed, and completing and reviewing the collection of information. Send comments regarding this burden estimate or any other aspect of this collection of information, including suggestions for reducing this burden, to Washington Headquarters Services, Directorate for Information Operations and Reports, 1215 Jefferson Davis Highway, Suite 1204, Arlington, VA 22202-4302, and to the Office of Management and Budget, Paperwork Reduction Project (0704-0188), Washington, DC 20503.

1. AGENCY USE ONLY (Leave blank)		2. REPORT DATE 19 July 1993	3. REPORT TYPE AND DATES COVERED Final: January 1986 to September 1990	
4. TITLE AND SUBTITLE Investigation of the Origin of Hot Spots in Deformed Crystals: Final Report on Ammonium Perchlorate Studies			5. FUNDING NUMBERS C - N00014-87-K-0175 C - N00014-85-WR-24103	
6. AUTHOR(S) W. L. Elban (Loyola College) H. W. Sandusky B. C. Beard B. C. Glancy (NSWCDD)				
7. PERFORMING ORGANIZATION NAME(S) AND ADDRESS(ES) Naval Surface Warfare Center (Code R13) 10901 New Hampshire Avenue Silver Spring, MD 20903-5640			8. PERFORMING ORGANIZATION REPORT NUMBER NSWCDD/TR-92/206	
9. SPONSORING/MONITORING AGENCY NAME(S) AND ADDRESS(ES) Office of Naval Research Code 1132P 800 N. Quincy Street Arlington, VA 22217-5660			10. SPONSORING/MONITORING AGENCY REPORT NUMBER	
11. SUPPLEMENTARY NOTES				
12a. DISTRIBUTION/AVAILABILITY STATEMENT Approved for public release; distribution is unlimited.			12b. DISTRIBUTION CODE	
13. ABSTRACT (Maximum 200 words) <p>A number of single crystals of ammonium perchlorate (AP) were shock loaded near the reaction threshold to investigate the effects of concentrated lattice defects (dislocations) and differing crystal orientations on chemical reactivity. Large, optical quality crystals of pure AP were immersed in mineral oil and shocked through either the (001) or {210} surfaces by a detonator. Prior to shock loading, some crystals had localized regions of increased lattice defects and strain created by placing diamond pyramid (Vickers) hardness impressions into their exterior cleavage surfaces. High-speed photographs showed preferential cracking and luminosity near some of the hardness impressions. The photographs also revealed the occurrence of the same slip deformation identified previously from hardness testing. The shocked crystals were recovered, sometimes intact, for microstructural characterization and chemical analyses. Crystal orientation relative to the shock propagation direction changed the dynamic response and threshold for decomposition of the crystal, indicating the influence of material microstructure. Similarly, placing the hardness indenter in various surfaces of unshocked crystals activated different slip and crack systems. One recovered crystal was cleaved twice through hardness impressions on the (001) and shock-entry (210) surfaces, allowing spatial analysis of the interior regions of the crystal using x-ray photoelectron spectroscopy (XPS). Along these freshly cleaved surfaces, the XPS results showed enhanced lattice disruption and perchlorate decomposition as a result of the hardness impressions. The greatest decomposition was not immediately adjacent to the impressions, but near the tips of cracks and along slip planes emanating from the impressions several millimeters, or more, into the crystal.</p>				
14. SUBJECT TERMS Ammonium Perchlorate Hot Spot Microhardness			15. NUMBER OF PAGES 41	
X-ray Photoelectron Spectroscopy Dislocation Density Shock Reactivity			16. PRICE CODE	
17. SECURITY CLASSIFICATION OF REPORT UNCLASSIFIED	18. SECURITY CLASSIFICATION OF THIS PAGE UNCLASSIFIED	19. SECURITY CLASSIFICATION OF ABSTRACT UNCLASSIFIED	20. LIMITATION OF ABSTRACT SAR	